Final Report on N64-18439*
(NASA Grant NsG-468) CODE-1
CR-53516

EVALUATION OF THE LUNAR PHOTOMETRIC FUNCTION

Final Report

Submitted by:
Hermon M. Parker,
Thomas T. Mayo, IV,
D. Scott Birney, Jr., and
George McCloskey

Jan. 1964 71 pp
refs

Submitted to:
NASA Langley Research Center
Hampton Station
Langley, Virginia

(3) Research Laboratories for the Engineering Sciences
University of (1) Virginia U.,
(2) Charlottesville

2398774

(NASA CR - - -;
Report No. AST-4015-101-64U) OTS:

January 1964

Final Report on
NASA Grant NsG-468

EVALUATION OF THE LUNAR PHOTOMETRIC FUNCTION

Submitted by:
Hermon M. Parker
Thomas T. Mayo, IV
D. Scott Birney, Jr.
George McCloskey

Submitted to:
NASA Langley Research Center
Hampton Station
Langley, Virginia

RESEARCH LABORATORIES FOR THE ENGINEERING SCIENCES
UNIVERSITY OF VIRGINIA
CHARLOTTESVILLE, VIRGINIA

Report No. AST-4015-101-64U

January 1964

Copy No. 4

ABSTRACT

A critical study of the available lunar photometric data has been made with the purpose of determining the accuracy with which lunar surface brightnesses may be predicted. Conventionally the brightness is expressed as $B = B_o \rho \phi$, where B_o is porportional to the solar flux, ρ is the albedo, ϕ is the photometric function, and ϕ depends upon the angles of incidence and emittance and by definition is unity for normal incidence and normal emission.

The best published set of data for lunar maria, Fedoretz [1], (used by JPL to determine a photometric function [7]) was used to determine the photometric function. The Fedoretz maria data plotted against brightness longitude (Figures A-1 to A-21) for constant phase angle were fitted to a) the Cornell theoretical photometric function [9], b) a theoretical photometric function based on a modification of lunar models used by Bennett [3] and Van Diggelen [8], and c) empirical hand-drawn curves through the data points. Procedure c) resulted in somewhat smaller root mean square deviations and provided a photometric function which was compared with that published by JPL. The comparison indicated that no significant change of the JPL photometric function is warranted. The rms deviations due to the scatter in the data indicated that for regions not closer than 20° to the limbs the photometric function may be expected to be accurate to within $\pm$ 10%. A dependence of the photometric function on brightness lattitude could not be detected.

The next best published set of data for lunar maria, Sytinskaya and Sharonov [2], was analyzed in the same fashion (Figures A-22 to A-31) and gave a photometric function which at some phases was considerably higher than ϕ derived from the Fedoretz data. Primarily due to the fact that the S and S data has no phase angles closer to zero than $g = +4.^\circ 6$ (as compared to $g = -1.^\circ 48$ for the Fedoretz data), less confidence can be placed in a photometric function derived from the S and S data.

The most frequently quoted list of measured albedos is that of Sytinskaya [10] and the values in some instances are means of a considerable range of indivisual observations. When maximum accuracy is desired,

the albedo for the particular feature should be used and if a reliable value is not available it should be independently determined.

A review of lunar surface slope determinations is given. The problem of slope determination from lunar satellite observations is considered. It is shown that if the photometric function is known, the surface slope can, theoretically, be determined. An error analysis for such slope determination has not been made.

TABLE OF CONTENTS

LIST OF ILLUSTRATIONS

LIST OF TABLES

SECTION I
INTRODUCTION

Many earth based studies of the moon's brightness have been made over the years, and the brightness of the integrated light of the entire lunar disc has been well established. Relative brightnesses of specific areas have also been determined for numerous cases, and observers have discovered the interesting and highly significant manner in which the surface brightness varies throughout each lunation. The mission to study the moon's surface from an unmanned satellite orbiting the moon introduces its own new problems. But the currently available brightness data can, nevertheless, be used to predict the ranges in brightness which the satellite cameras will encounter. We hope to show here the accuracy which may be expected from such predictions.

SECTION II

BASIC DEFINITIONS

Following are a few of the basic definitions which will be used in the subsequent discussion. These are included to insure uniformity and consistency.

Angle of incidence, i - the angle between the normal to the surface and the incident ray.

Angle of emittance, ϵ - the angle between the normal to the surface and the direction of the emitted ray.

Phase angle, g - the angle at the center of the moon between the directions to the sun and the earth. This is also, of course, the angle between the incident ray and the emitted ray at any point on the surface. The phase angle may vary from -180° at new moon to 0 at full moon and +180° after full moon.

Sub-sun point, S_s - the intersection of the line between the centers of the sun and moon with the surface of the moon.

Sub-earth point, E_s - the intersection of the line between the centers of the earth and moon with the surface of the moon.

Selenographic Longitude, λ - the angle measured along the moon's equator from the mean center of the moon's disc to the great circle passing through the moon's poles and the point in question. λ is positive in the direction of Mare Crisium.

Selenographic Latitude, β - the angle measured northwards (+) or southward (-) from the moon's equator to a point on the surface along the great circle through the point and the poles.

Brightness equator - the great circle passing through the sub-earth and sub-sun points.

Brightness longitude, α - the angle measured along the brightness equator between the sub-earth point and the normal projection of the surface point onto the brightness equator. By convention α is positive in the direction away from the sun.

Brightness latitude, β_B - the angular distance of a surface point north or south of the brightness equator.

Albedo, ρ - ratio of the luminance of a surface under normal illumination and normal emittance to the luminance of an ideal white surface under normal illumination and normal emittance.

Photometric function, ϕ - a function by which is given the dependence of the brightness on the geometry of the particular situation being considered. That is, ϕ depends in some complex way on the angles of incidence and emittance and the phase angle. It varies from 1.0 at full moon to zero at larger phase angle.

Limb - the edge of the apparent disc of the moon.

Terminator - the line separating the illuminated and dark portions of the lunar surface.

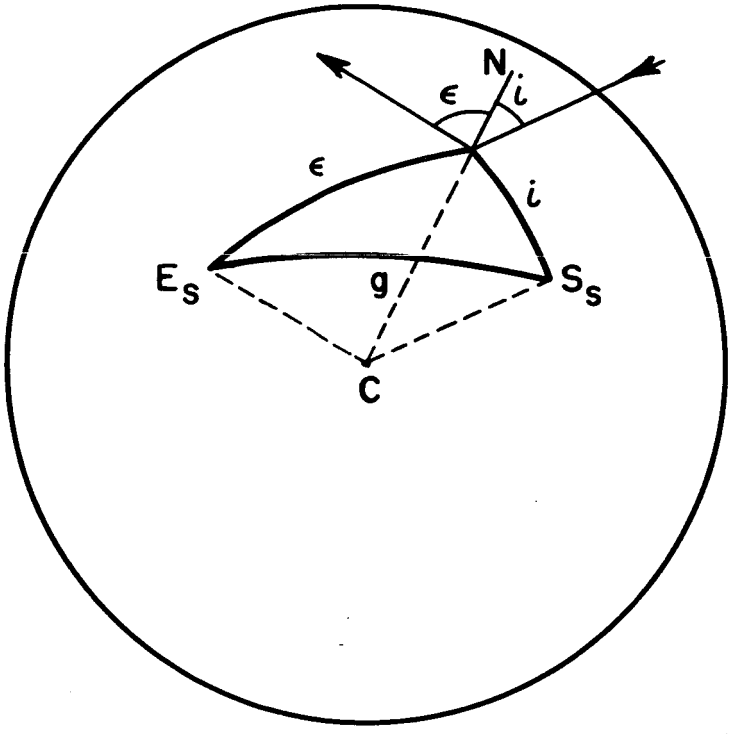

FIGURE-1

GEOMETRY OF OBSERVATION OF THE

LUNAR SURFACE

SECTION III

BRIGHTNESS VARIATIONS AND THE PHOTOMETRIC FUNCTION

The brightness of a particular region on the moon depends upon three factors: the nature of the surface itself; the intensity of the illumination; and the angles at which the surface is illuminated and viewed. This may be expressed as:

$$B = B_o \rho \phi$$

where the various factors are defined above or as follows:

B = observed brightness

B_o = normal surface brightness = $\frac{1}{\pi} E_s$

(E_s = the solar constant = 1.4×10^6 ergs/cm^2/sec outside the earth's atmosphere).

Brightness measurements made at a number of phase angles before and after full moon may be plotted against phase. Typical of such curves are the two shown in Fig. 2 for areas in two seas. In absolute units, the peak value of such a curve depends on the albedo of the area studied. Beyond this, however, the form of the curves depends on the photometric function ϕ. Two points are worthy of note. First, the curves show a rapid increase and a rapid decrease before and after full moon. Second, at full moon, the moon appears uniformly bright when surfaces of a similar albedo are compared in various parts of the disc. The assymetry of the curves results from the location of points either east or west of the central meridian of the moon.

Clearly this is not the way in which a smooth uniformly-diffusing spherical surface (Lambert sphere) will reflect light. For many years, therefore, it has been generally accepted that the photometric properties of the moon somehow resulted from the detailed structure

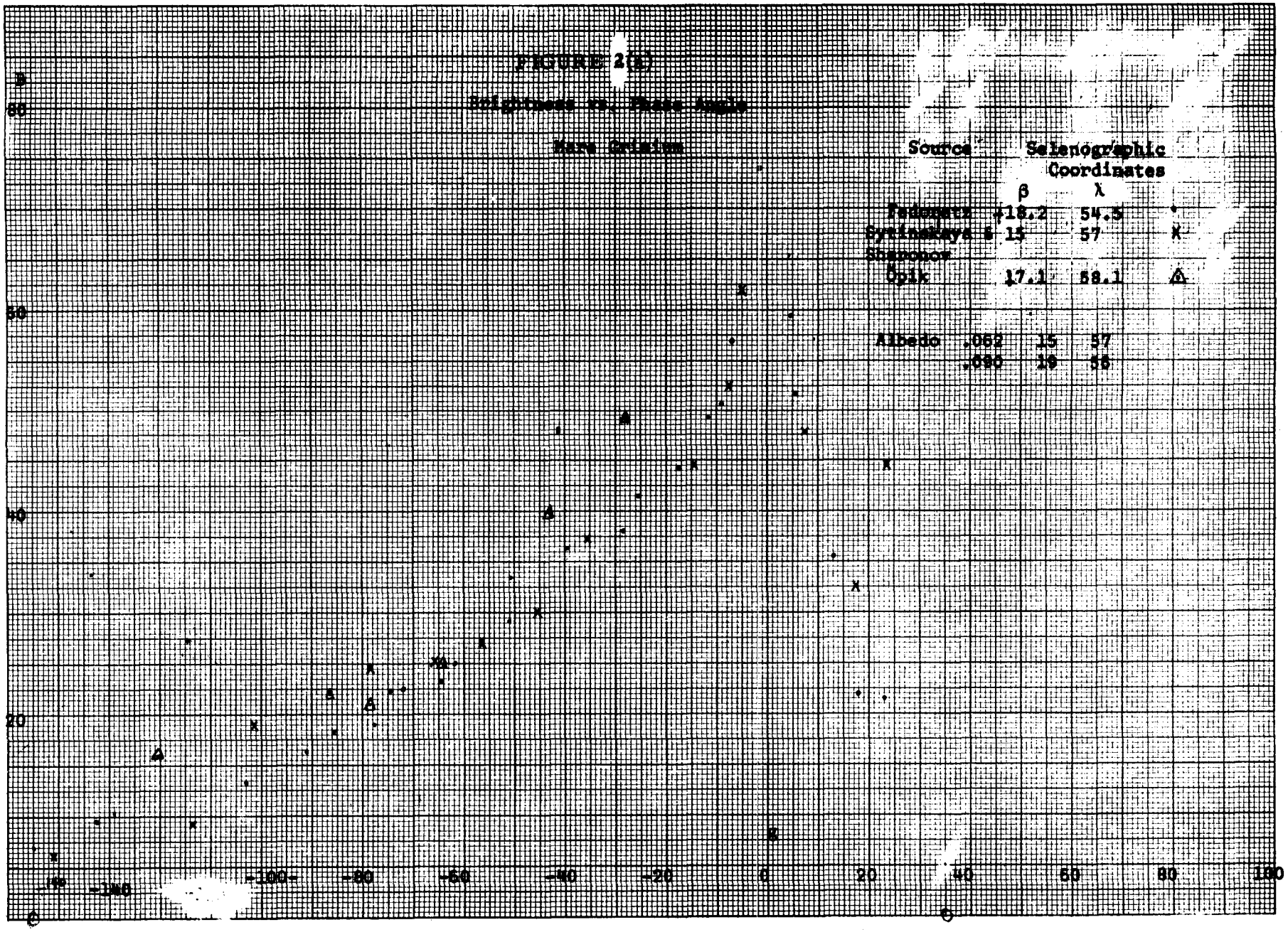
FIGURE 2(a)
Brightness vs. Phase Angle
Mare Crisium
Source
Selenographic Coordinates
β
λ
Fedorets +18.2 54.5
Cytinskaya 15 57
Shapopov
Opik 17.1 58.1
Albedo .062 15 57
.090 19 56
80
60
40
20
-100
-80
-60
-40
-20
0
20
40
60
80
100

FIGURE 2(b)
Brightness vs. Phase Angle
Mare Nectaris

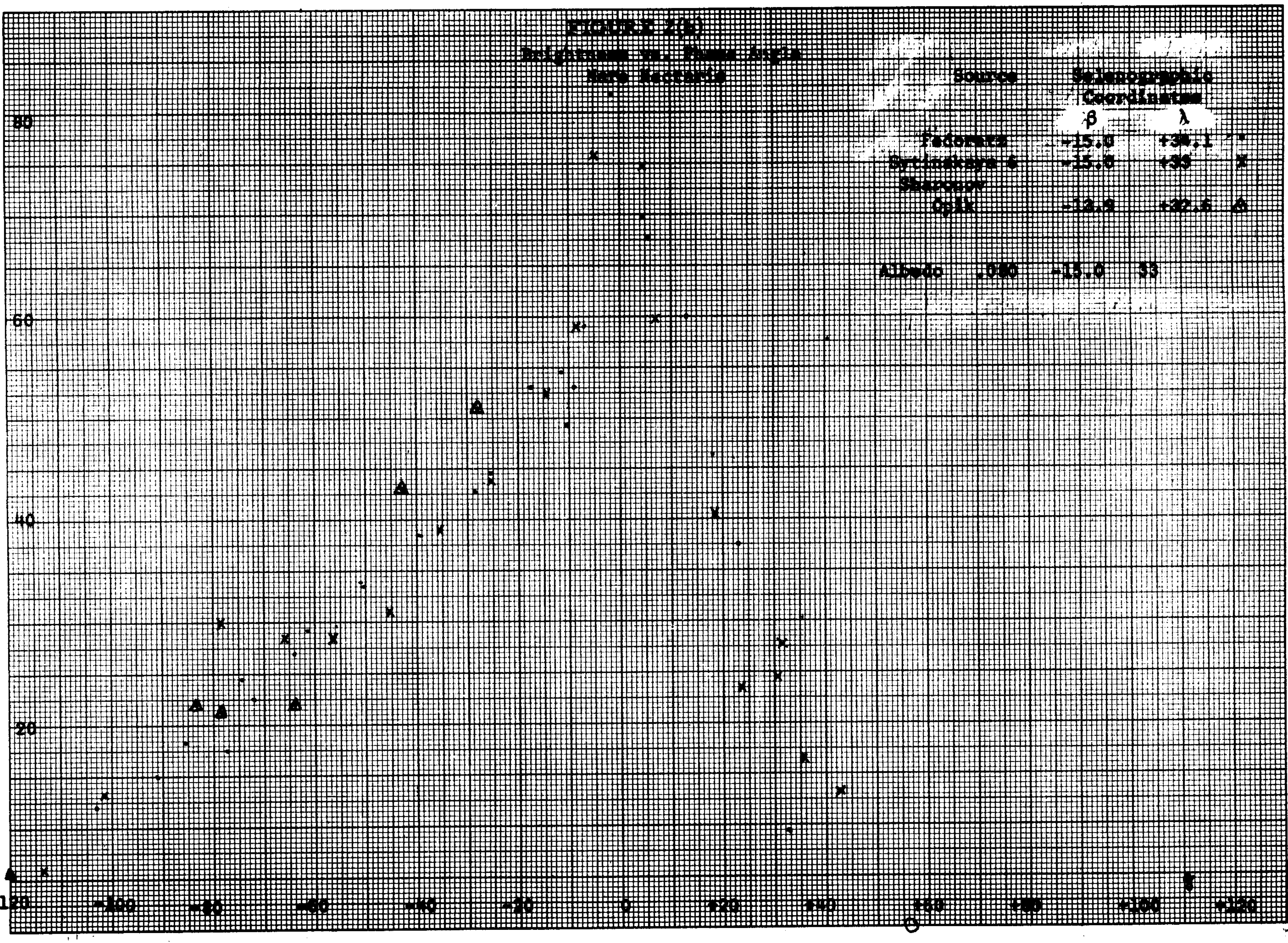

of the lunar surface. Extensive laboratory tests have been made by several investigators to find a common terrestrial material which would not only show an albedo comparable to those on the moon but would also reproduce the observed phase-brightness effects. The material which shows the best fit to the lunar brightness curves is volcanic tuff. In addition, theoretical surfaces of several geometrical configurations have been studied analytically in an effort to find a surface that accounts for the moon's observed photometric properties. These models usually assume a surface covered to some degree with small depressions. Two such theoretical models will be discussed in Section VII.

In the present study, the importance of the photometric function lies in the fact that the predicted brightness of a given lunar area depends significantly on the photometric function. If the correct value of the exposure for either a television or a photographic camera is to be known in advance, the photometric function must be known as accurately as possible. Extensive series of photometric observations have been published by several investigators (see Table I). Of these observations, only those of Fedoretz, Systinskaya and Sharonov, and Fessenkov are complete enough at numerous phases to warrant extensive consideration in this study. It has thus been our purpose to evaluate critically the available data and the photometric function as it has been previously derived from this data.

SECTION IV

PROCEDURE FOR THE REDUCTION OF PUBLISHED OBSERVATIONS TO FIND THE PHOTOMETRIC FUNCTION

It has been shown elsewhere [13] that the photometric function depends very little, if at all, on the brightness latitude of the point considered. Because of this it was decided to plot the photometric function against brightness longitude, α, for each phase. When the photometric function is displayed in this fashion, it should be possible to detect its variation with latitude by finding the correlation between the latitude of points with nearly the same longitude and the value of their photometric function for selected phases, (i. e. one looks for scatter which results from latitude differences).

This mode of displaying the photometric function derived from the published data requires the determination of the brightness coordinates, α and β_B, for each point considered. The selenographic coordinates measured with respect to the moon' s equator must be referred to the brightness equator which depends on both the phase and positions of the Earth and sun with respect to the true equator at the time of the observations. The extensive labor involved in actually carrying out this coordinate change was considerably reduced by programming the problem for the Burroughs 205 Computer at the University of Virginia.

Let $D_i(g)$ be data given by a particular paper for the i^{th} feature at phase g. In general,

$$D_i(g) = B_i \phi (g, \alpha)$$

where B_i is the proportionality constant between the data and the photometric function and α is the brightness longitude of the i^{th} feature at the time of observation. B_i should vary from feature to

feature as the albedo varies and from author to author depending on how their data was obtained. In all cases treated here, the approximate photometric function ϕ_a was found by,

$$\phi_a = \frac{D_i(g)}{D_i(g_s)}$$

where both pieces of data are taken from the same source in the literature and g_s is the phase nearest full moon reported by that source. In using this as an approximation it is assumed that the B_i values are the same for the two pieces of data so that,

$$\phi_a\ (g, \alpha) = \frac{\phi(g, \alpha)}{\phi\ (g_s, \alpha')}$$

where α is not necessarily equal to α' due to the moon's libration. (This, however, should introduce little error since for g close to zero, ϕ becomes independent of α.)

This convenient approach aleviates the necessity of determining the proportionality between the data and the true brightness. Further, it makes it possible to obtain values for the photometric function for features whose albedos are not known. It also may serve to remove systematic errors which result in the data not having the proportionality to photometric function which is indicated by the description of the experiment. On the other hand, this procedure can introduce error in the resulting photometric function, since the brightnesses used are not actually those for full moon. This error will be discussed later.

SECTION V
PHOTOMETRIC FUNCTION FOR THE LUNAR MARIA

We proceed now to derive and display a photometric function for the lunar maria. To do this we must make use of observed values of brightness or relative brightness at a wide variety of phases for a collection of points well distributed over the maria. The published sources which best fulfill this requirement are given in Table I.

TABLE I

	Number of Phases	Number of Points in Maria
Fedoretz 1952 [1]	40	41
Sytinskaya and Sharonov 1952 [2]	41	26
Bennett 1938 [3]	11	20
Fessenkov, Parenago, and Staude 1928 [4]	13	many but different for each phase

Fedoretz

Figure 3 and those in the Appendix show Fedoretz' s data for selected phases treated as described above. It will be noticed that the range in longitude over which there are data points ends at least twenty degrees from each limb. This not only results in each curve being incomplete but also in it being impossible to obtain meaningful curves for large positive and negative phase angles.

The drawn curves represent a visual estimate of a best fit to the data. (Though they are not included in this report, the brightness latitude of each plotted point was calculated and the scatter of the data about the drawn curves was examined in light of these. Latitude values as high as 64° were obtained. However, no correlation was detected.)

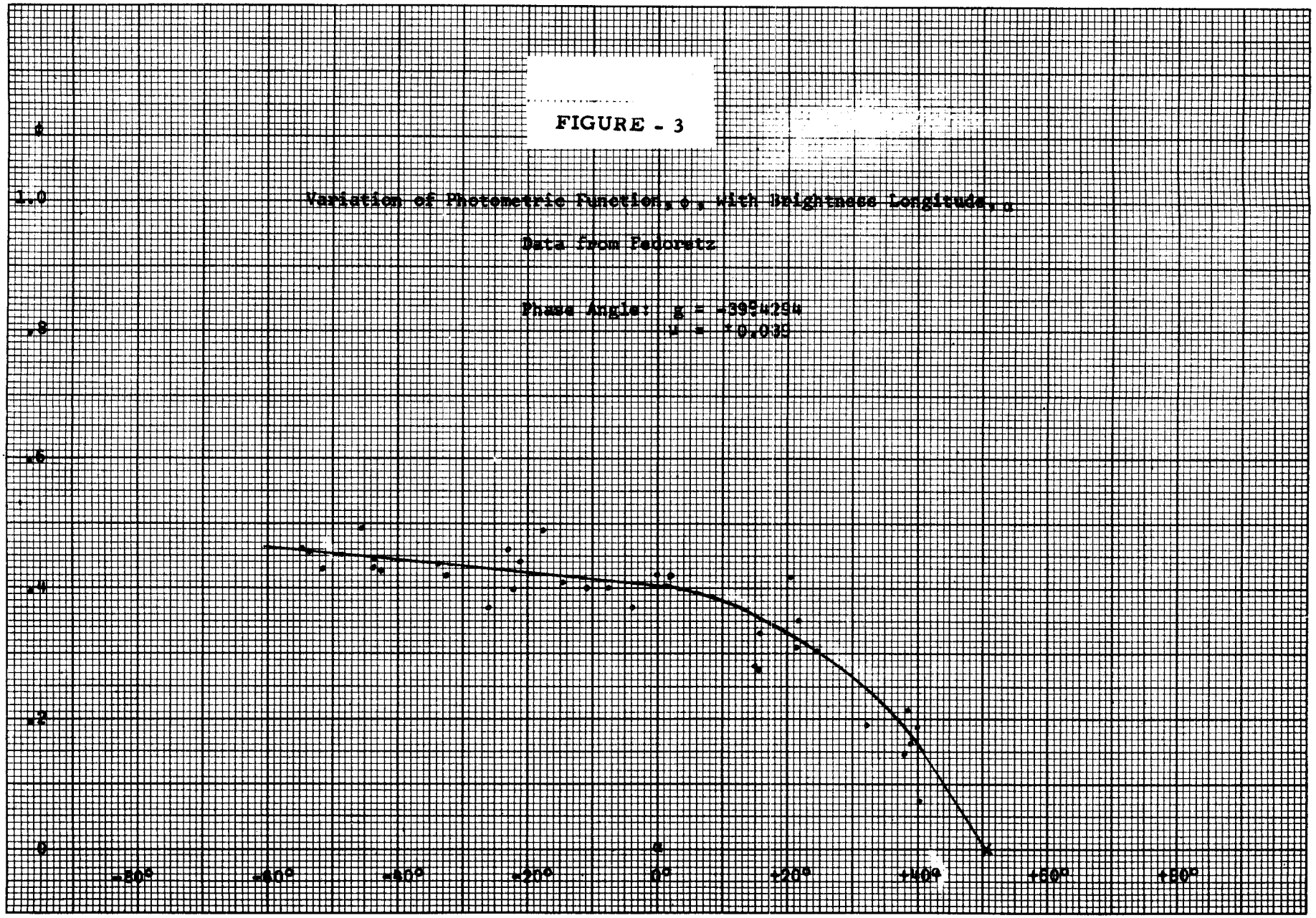
FIGURE - 3
Variation of Photometric Function, Φ, with Brightness Longitude, α
Data from Fedorets
Phase Angle: g = -39°.794
ψ = +0.032
Φ
1.0
.8
.6
.4
.2
0
-80°
-60°
-40°
-20°
0°
+20°
+40°
+60°
+80°

The μ values given on the figures are the root mean squared values of the deviations from these hand-drawn curves. These values are generally about 10% of the maximum value of the curve.

The lunar feature brightnesses used in the place of those for full moon came from a phase of -1.°48. This data is from a photograph made by Fedoretz just before an eclipse of the moon, and is about as close to zero phase as one can hope to go. The average effects of this choice can be estimated by finding the percent difference between the values at full moon and at a phase of -1.°48 on the brightness-phase curve for the integrated light of the whole moon as published by Rougier [6]. This percentage difference is about 1% indicating that on the average our plotted points are about 1% too high. Variations in the size of this effect from features of one type to another would be important and consequently such variations were looked for. Published albedos for sixteen of Fedoretz features were found and these were combined with the brightness data at phase -1.°48 to give values of ϕ for the various features. All resulting values for ϕ were multiplied by the same constant to make their average 1.0. The values for the photometric function adjusted in this manner varied from 1.28 to 0.80. A plot of these values against α, the brightness longitude however showed no discernable correlation between ϕ and location of the point with respect to the sub-earth point. Such a correlation would have suggested that the data from phase -1.°48 had introduced a systematic error.

Sytinskaya and Sharonov

In some cases the curves of ϕ versus α for Sytinskaya and Sharonov's data lie considerable above those for Fedoretz at the same phase. It has occurred to us that this may be understandable if the part of the moon for which the photometric function seems to be too large is consistently on the side of the sub-earth point away from the sub-sun at phase g_s, since the effect of g_s being other than zero (in this case +4.°6) would be greatest there.

Unfortunately, we have not been able to explain the fact that the Sytinskaya and Sharonov curves are higher than Fedoretz' curves. Therefore, we have not tried to combine the observations of the two groups.

Others

The data produced by Fessenkov et al and by Bennett is very difficult to handle because neither publication contains phases very close to full moon. Also in both of these cases the data is made somewhat inaccessible by the use of obscure systems for locating the data points on the lunar surface. Bennett uses points identified by Nieson in his book The Moon (LONDON, 1876), (which we have not been able to locate) and only refers to them by Nieson number. Fessenkov referred the points for which he has data to a different rectangular coordinate system at each phase and seems to have made no effort to take data for the same lunar feature at different phases. Presumably, the difficulties for both of these could be overcome. However, it is quite unlikely that data could be obtained for as many lunar features as would be necessary in order to make a significant contribution to the determination of the photometric function for the lunar maria.

SECTION VI

A COMPARISON OF THE PHOTOMETRIC FUNCTIONS OF UVA AND JPL

Previously a photometric function derived from Fedoretz' s data has been published by JPL [7]. Apparently JPL has interpolated between the actual curves since their published curves are at 10 degree intervals in phase and Fedoretz data is for irregular phases. Values of ϕ for comparison with the curves in this paper were obtained by a linear interpolation between JPL' s curves. It is estimated that the maximum error in obtaining these values is $\pm$ 0.02. The interpolated values minus the corresponding value from the curves in this paper may be found in Table II.

Since JPL claims to have been conservative in the values for the photometric function, only those points for which the difference is positive and greater than (+ 0.02) should be of very much concern. Such values only occur for negative phases. Apparently JPL' s curves are conservative compared to the average of the curves for equal positive and negative phases. However, if the difference between equal positive and negative phases displayed here is real, a better conservative choice for the photometric function might be the curves for the negative phases. In any case, if one remembers that the μ values are about 10% of the maximum value for each curve, it is not difficult to estimate the significance of the percentage difference between the two sets of curves.

TABLE II

DIFFERENCES BETWEEN THE JPL PHOTOMETRIC FUNCTIONS AND THE PHOTOMETRIC FUNCTION DERIVED DIRECTLY FROM FEDORETZ' DATA, JPL MINUS F

Brightness Longitude, α	Phase, g: -90°.6	-77°.4	-64°.2	-51°.1	-39°.4	-28°.5
-60	+.02	+.06	+.05	+.04	(+.02)*	-
-40	+.02	+.03	+.01	+.03	+.00	+.07
-20	+.02	+.04	+.02	+.01	+.00	+.07
0	-	+.02	+.01	+.00	-.02	+.01
+20	-	-	-	+.01	-.03	-.02
+40	-	-	-	-	-.06	-.03
+60	-	-	-	-	-	-
μ**	.01	.02	.03	.04	.04	.05

α	-17°.9	-9°.0	+4°.5	+17°.8	+42°.9	+74°.3	+87°
-60	(.16)*	-	-.06	-.15	-.12	-.11	-.02
-40	+.08	+.15	-.05	-.18	-.12	-.07	-.01
-20	+.05	+.05	-.05	-.18	-.06	-.01	+.01
0	-.02	-.03	-.01	-.18	-.03	.00	-
+20	.00	-.08	+.02	-.20	+.01	-	-
+40	-.09	-.12	(+.04)*	-.16	-	-	-
+60	-	-.15	-	-	-	-	-
μ**	.04	.08	.09	.09	.03	.02	.02

* Values in parenthesis were obtained by performing extrapolations of the curves in this paper.

** μ is the rms deviation of the plotted points from the hand drawn curves in Figure 3 and in the Appendix.

SECTION VII

THEORETICAL PHOTOMETRIC FUNCTION

It is difficult to fit a meaningful curve to a collection of data when the scatter in that data is fairly large, unless the type of function which the data should follow is known from theoretical considerations. Since the lunar photometric data does contain considerable scatter, it is desirable to attempt to find such a mathematical function for it.

Until recently the most successful attempts in this direction had been made by Bennett [3] and Van Diggelen [8] on the basis of the moon's being a Lambert sphere partially covered with hemi-spherical or hemi-ellipsoidal holes of small dimensions. Bennett's approach was to find an expression for the illuminated fraction of the visible area inside a hemi-spherical hole when this area is projected normal to the direction of emittance.

This expression multiplied by the fraction of the lunar surface covered with holes was then added to the cosine of the angle of incidence multiplied by the fraction of the surface not in holes to produce a function proportional to the photometric function.* Bennett's final expression is,

$$h = h_o (C \cos i + (1-C)V)$$

where h = surface brightness, h_o = surface brightness for phase angle of 0°, i = angle of incidence, C = fraction of surface which is smooth and V = illuminated fraction of holes' projected area.

---

* In finding the illuminated fraction of the holes' projected area, a change of coordinate is made by Bennett which seems to result in the calculated visible illuminated projected area being too large by a factor, $(\cos \epsilon)^{-1}$. The fact that Bennett apparently overlooked this may help explain why the resulting function seems to be good only close to the sub-earth point.

Bennett also made an estimate of the improvement in matching his data that he might obtain from considering hemi-ellipsoidal holes.

It occurred to us that to be consistent, the holes also should be considered Lambert surfaces. This means the true cosine of the angle of incidence in a hole, averaged over the area of the hole, projected normal to the direction of emittance, should replace the illuminated fraction of the hole's projected area in Bennett's expression for the photometric function. It also occurred to us that the calculation of a photometric function from this model would be simplified considerably if it were carried out for points on the brightness equator only.** Such procedure, if successful, would yield a useful function, since the lunar photometric function seems to be independent of brightness latitude.

The resulting function is,

$$\phi = A\{C\cos i + \left((1-C)/3\pi\cos\epsilon\right)[2(\pi-g-i-\epsilon)\cos g + \sin(2i+g) + \sin(2\epsilon+g)]\}$$

where A is a proportionality constant, (1-C) is the fraction of the moon's surface in holes, and $0 \leq g \leq \pi$. It is easy to see with ϕ written in this form that it obeys reciprocity (i.e., $\phi(\epsilon, i, g)/\phi(i, \epsilon, g) = \cos i/\cos\epsilon$, a condition which is established as necessary for all photometric functions by thermodynamic considerations)[13]. However, the less ambiguous form for ϕ in the case of this model is as a function of g and α rather than i, ϵ, and g. For a point between the terminator and the sub-earth point,

$$\phi_1 = A\{C\cos(g+\alpha) + \left((1-C)/3\pi\cos\alpha\right)[2(\pi-2g+2\alpha)\cos g + \sin(3g-2\alpha) + \sin(g+2\alpha)\}.$$

For the points between the sub-earth and the sub-sun points,

$$\phi_2 = A\{C\cos(g+\alpha) + \left((1-C)/3\pi\cos\alpha\right)[2(\pi-2g)\cos g + \sin(3g-2\alpha) + \sin(g+2\alpha)]\}$$

**Van Digellen [8] in his attempt to determine from this model a photometric function for points apparently off the brightness equator, was forced first to a numerical approach and then to experiment.

For points between the sub-sun point and the limb,

$$\phi_3 = A\{C\cos(g+\alpha) + \left(2(1-C)/3\pi\cos\alpha\right)[(\pi-2\alpha)+\sin\alpha]\cos g\}.$$

It is not difficult to show that this function does not have the desired property of being maximum at full moon. (Consider the fact that the first term in it is maximum at full moon only for the sub-earth point.) It is also obvious that at full moon the function varies with brightness longitude. Nevertheless, attempts were made to adjust A and C by the method of least squares so that it would fit the photometric function derived from Fedoretz's data. This was done at phase angles -145.°29, -132.°49, -128.°56, -102.°79, -90.°58, and -25.°60. For the first five of these, this amounts to fitting AC cos i to the data, since for phase greater than 90° in magnitude the holes along the equator do not appear illuminated. A reasonably good fit was obtained for all these. At -25.°60 so much loss of accuracy occurred in the calculation that no meaningful values for A and C could be obtained simultaneously. By making arbitrary choices of C and calculating A by the method of least squares it was discovered that the root-mean-squared deviation of the data points from the fitted curve is not a strong function of C, and that all values of C less than 0.2 produced almost equally good fits to the data ($\mu \cong 0.057$). These results together with the deficiences in the general properties of the function were sufficiently discouraging to halt efforts along this line.

It is worth mentioning here, perhaps, that during the period of the grant supporting this work, a group at Cornell University in a report to NASA [9] published a new theoretical photometric function which is probably the best to date. The model assumes that the moon's surface is a spherical shell of freely suspended back scatterers. The resulting function is the product of three factors: one which arises from considering the probability of interaction between scatterers at a given depth below the surface with both the entering and leaving light; second, a back scattering function; and third, a factor which takes care of the increased probability of no second scattering after back scattering. The first of these is the Lommel-Seliger Law, $\frac{\cos i}{\cos i + \cos\epsilon}$,

and the last two of these are strictly functions of phase angle, both containing adjustable parameters.

In keeping with this approach we have done a least square fit of the Lommel-Seliger Law multiplied by an adjustable parameter to two phases, -25.°60 and 42.°87. The root-mean value for the deviations about the resulting curves were 0.054 and 0.046, respectively.

We have not developed sufficient confidence in either of these theoretical models to use one to represent the reduced data presented here.

SECTION VIII

MEASURED ALBEDOS

The most commonly employed practice for determining albedo involves simply the manipulation of brightness observations made as near as possible to full moon. The value of the photometric function at full moon is 1.0 for all points. Therefore, the relative brightnesses of various areas at full moon depend on the albedos of the areas in question. For the case at full moon, we may write.

$$\rho = B/B_o$$

or,

$$\rho = B/(E_s/\pi)$$

Full moon albedos may thus be determined simply by dividing the observed brightness of a point by the normal surface brightness. In practice there will always be observational errors in the brightness values. This introduces some uncertainty especially if there is only limited data available. More important as a source of uncertainty, however, is the fact that observations can never be made at a phase angle of precisely zero degrees and few observations at phase angles near zero degrees are currently available. This means that the required value of B to be used in the equation above is never actually observed. It must always depend upon the curve drawn through observed points at greater phase angles. The uncertainty in B is easily seen in Figure 2 in which data from several observers has been plotted.

From the fact that all curves such as these rise very steeply near zero phase, it is clear that points as close to zero phase as possible are very important. Fortunately, as stated above, Fedoretz

was able to obtain observations just before a lunar eclipse when the phase angle was -1.°48. These values are undoubtedly very close to the true zero-phase brightnesses. The point here is emphasized by the case of Mare Crisium (Figure 2) in which the point for -1.°48 is surprisingly high compared to the points closest to it in phase. Clearly, the calculated albedos will embody any errors which may arise from these two sources.

Sytinskaya [10] has assembled a list of albedos determined by four observers for 104 features. The agreement between the four values for individual features is of the order of 5 percent and the means of the four values are also included in her table. Sytinskaya has also grouped the features according to type (i. e. maria, bright plains, mountains, craters and bright rays) and determined average albedos for each class of features. This summary list is the one most frequently quoted throughout the current literature, and these means are undoubtedly good representations of the albedos. However, some care should be used in applying these albedos in any situation requiring great accuracy. One reason for this is the range in values incorporated into the means for individual points. For most of the points in Sytinskaya' s list the extreme values are not further than 0.003 from the mean of the four values. For the worst case, however, the values range from 0.040 to 0.075 around the mean 0.062. A second reason for preceding with care comes from the fact that there is again some spread around the mean when the approximately thirty albedos are averaged to find the mean albedo of all maria. This average, however, includes values ranging from 0.056 to 0.073. This means that when an albedo is used along with other factors to compute a predicted brightness in some areas, the predicted brightness may be in error by plus or minus ten percent. For the best predictions of absolute brightness, then, it is necessary to use albedos for the particular areas in question rather than the averages for the various classes of features. Where reliable albedos are not currently available, they should be independently determined before being used in situations requiring great accuracy.

SECTION IX
THE RANGE IN MEASURED SLOPES

The brightness of a surface under some given illumination varies with the cosine of the angle of incidence of the light. Thus, as the angle of incidence becomes large, small changes in $\underline{i}$ produce relatively larger changes in brightness. In the case of the moon, then, differences in slope result in differences in $\underline{i}$ for adjacent regions. These differences in $\underline{i}$ result in turn in differences in brightness.

One may see readily from the geometry of the situation and the definitions of g and α that the angle of incidence of the light at given points on the surface depends on both the phase angle g and the brightness longitude α measured from the sub-earth point. (As we have said earlier, there is no noticeable variation depending on brightness latitude). Therefore, whatever the phase of the moon, the angle of incidence will be smallest near the sub-sun point and will become larger as the combination of g and α becomes larger. Near the terminator i must necessarily be large and small differences in slope result in noticeable differences in brightness. As the terminator moves across the face of the moon, many otherwise invisible features become visible for short periods of time. This is essentially the conclusion reached in an analysis in terms of shade relief.

Shadows are, of course, most noticeable along the terminator, but we are not concerned here with shadows. We consider only the variations in brightness resulting from differences in the angle of incidence of the light.

From this, it should also be clear that a ridge running in a north-south direction will be more easily detected than will a ridge running in an east-west direction. The angle of incidence of the light falling on the north-facing slope will be the same (or very nearly the same) as the angle of incidence of the light falling on the south-facing slope. Therefore differences in brightness for these slopes are not likely to be very obvious.

The inclinations of gross slopes such as those in the maria have been measured in several ways [11]. The simplest method of studying these slopes is to observe at the proper phase the shape of the

terminator as it crosses the area in question. The terminator should appear as an ellipse if the Moon is spherical. Departures from sphericity will be seen as departures of the terminator from the ideal ellipse. The slopes detected in this way are of the order of 2° at the most even in the so-called "wrinkled" areas.

Slightly steeper slopes averaging from 3° to 8° are to be found on the outer sides of crater walls. The inner sides of crater walls show slopes near 30° with steeper slopes associated with the smaller craters. These may be measured primarily from the shadows cast by the crater walls.

Near the limb of the Moon, slopes along very small arcs (200 feet) have been measured from the manner in which the light of a star diminishes as the star passes behind the limb. Slopes in the range from 1° to 18° have been measured but the exact types of features represented are not specified. These are average slopes over the interval in question and so this method by itself does not provide much information regarding the slopes over small intervals. These occultation studies were made on stars of large diameters. Further information possibilities would accompany occultation studies of point source stars. But no detailed results in this area are available.

A method of measuring slopes photometrically has been developed by van Diggelen and applied by him [12] to two areas in the Mare Imbrium.

On photographs of the Moon, van Diggelen has scanned selected areas at intervals corresponding to about 2" on the moon' s image. Scans across ridges show brightness changes and these are calibrated against scans across apparently smooth areas in the same vicinity. When the proper corrections have been applied, a curve representing variations in slope with distance is obtained. Integration of this curve gives the profile of the section through the ridge.

Profiles thus obtained are all approximately parallel to the Moon' s equator. And when a number of such profiles are combined for a given area, it is possible to draw a contour map of the area even though the ridge may not run in a predominantly north-south direction. From the contour map, of course, an idea of the slopes in north-facing and

south-facing directions may in many cases be obtained. It is from these studies that van Diggelen has concluded that even in the wrinkled areas, the slopes within the Maria are less than one part in forty over distances of three to five kilometers.

It would seem significant to ask how this method would apply in the lunar satellite situation in which photographs of smaller areas become available with better resolution. All of the above mentioned factors should apply just as they do for the larger areas visible from the earth. Variations in slope should result in variations in surface brightness for areas near the terminator. The reduction procedures used by van Diggelen no longer apply, however, because over a small area, a mile or so across, differences in slope due to the curvature of a smooth surface are too small to be noticeable as differences in brightness. Thus no ready means for calibrating the brightness variations in terms of slope is available. Some other scale of relative intensities must be provided.

SECTION X

SLOPE DETERMINATION FROM LUNAR SATELLITE OBSERVATIONS

Another theoretical approach to this problem of slopes becomes possible in the orbiting satellite situation. The geometry of an observation of a surface point, O, from a satellite is shown in Figure 4. The point S_s is the sub-satellite point. The brightness equator does not pass through S_s, however, because of parallax effects resulting from the relatively small height of the satellite above the moon's surface. A point G corresponding to the sub-earth point and lying on the brightness equator may be easily found.

For earth-bound observations, the sub-earth point may be defined either as the intersection of the Moon-earth line of centers with the lunar surface or the intersection with the lunar surface of a lunar radius parallel to the emitted ray being observed. For close lunar satellites the two definitions are not equivalent, so the question of how to define a brightness equator arises. However, on the assumption that one wishes to use information about $\phi(\alpha, \beta, g)$ determined from earth-bound data, the latter definition above must be used. Thus, in the satellite case, a radius CG is constructed parallel to the emitted ray from O to the satellite. SG then is the brightness equator for the point O and that position of the satellite in the sense that α, β and g are the appropriate ones to put into $\phi(\alpha, \beta, g)$ for observing O from the satellite.

Thus, for a particular satellite situation α and β may be determined. Knowing g and α, a value for ϕ may be obtained from the results of earth bound observations. The surface brightness may then be predicted for any point on the surface for a particular situation. If the surface normal at the point in question does not coincide with a radius of the sphere (i. e. if the local surface has a small scale slope in some direction), the observed brightness will be different from that predicted. The observed brightness in turn may be used to find an α_ϕ, a sort of photometric α from the

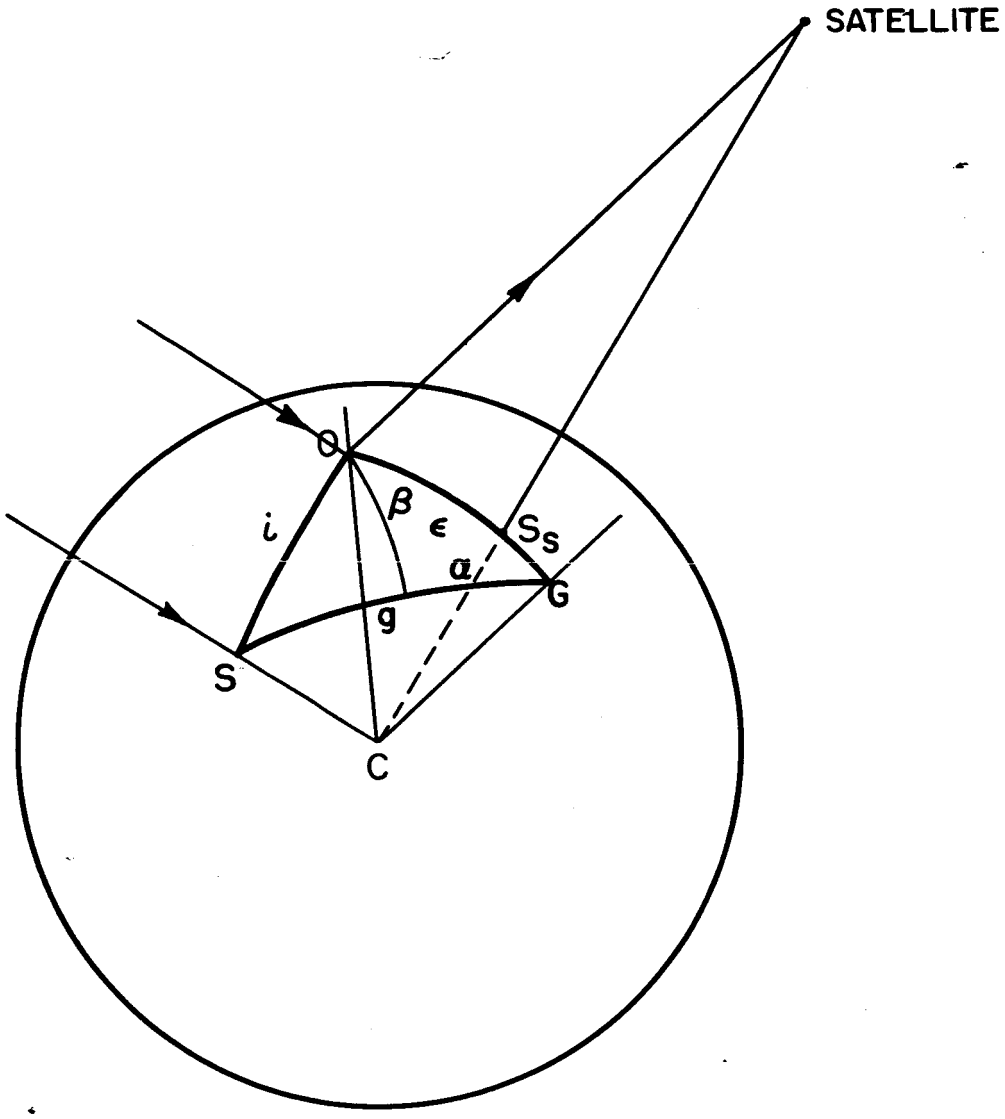

FIGURE–4

BRIGHTNESS COORDINATES IN THE LUNAR SATELLITE SITUATION

previous determination of ϕ vs. α. If along the brightness meridian α_ϕ, one could locate the point P' at which the radius P'S is parallel to the true surface normal at point P, then the angular distance between points P and P' is equal to the slope of the surface at point P which is being observed. A single observation gives only the α_ϕ of the point P' and defines only a great circle on which P' must lie.

As the satellite moves to a new position, a second observation of the same area can be made. For this situation there will be a new brightness equator and a new α and β. Thus a second great circle passing through P' may be found. If the coordinates of the intersection of these two great circles can be found in selenographic coordinates or in brightness coordinates with respect to either the first or second brightness equator, the local slope of the particular area may be known. This procedure is theoretically capable of giving the slopes of various areas even when the resolution of surface detail has become very good.

Some of the pitfalls or weaknesses are obvious. First, we must assume here that the photometric function is known to a high degree of accuracy. Second, the position of the satellite at the time of the photograph must be known precisely since g and α depend on this. Third, the two exposures must be as nearly identical as possible as that the data from the two may be combined.

Some time has been devoted to this analysis in order to insure that a solution is theoretically possible. However, no attempt has been made to evaluate the accuracy of such a solution in terms of the accuracy of the currently accepted photometric function and the parameters of the satellite's orbit. This in itself is an extensive undertaking.

SECTION XI
CONCLUSIONS

In the course of this program the available data from as many sources as possible have been studied and there seems to be little doubt that the best data on the surface brightness of the moon is that published by Fedoretz. Her data are more complete than that of any other observer, and all indications are that the data are self-consistant and that the observations were carefully made. From this data, then, a useful photometric function may be derived. As we have shown, there is considerable scatter in the data when photometric function is plotted against brightness longitude for various phase angles. It is difficult to know whether or not this scatter is real or results from observational errors. In attempting to fit a meaningful curve through the data points we have tried to find a theoretical function. We conclude, however, that there is no very good alternative to a hand-drawn curve through the plotted points.

The curves presented in the appendix represent the reduction of Fedoretz data and may be used to find a value of the photometric function for points in the maria under various phases. It is, of course, to be expected that interpolation between these curves will be necessary.

Calculated values of surface brightness require knowledge of the albedo of the area in question as well as the photometric function and for the highest degree of accuracy one should try to use the actual measured albedo for the given area rather than the albedo for a particular class of areas.

The question regarding the detection of slopes facing principally in the north or south direction has been examined also, and we point to the work of van Diggelen in which he determines east-west sections through irregular areas. When a series of such sections are assembled the contours of the area in all directions are readily seen. Applied to large areas near the terminator this method is effective. Over the small areas one might view from a satellite or in areas not near the terminator when photographed, van Diggelen's method cannot be applied without modifications.

Finally, this study suggests the need for additional work along two lines. Accurate determinations of albedo in numerous areas particularly within the maria may help to reveal the source of the observed scatter in the photometric function. One would hope also that improvements and extensions of the photometric function might be achieved by careful attention to the actual measurement of the photographs. Detailed studies of a few small areas might be undertaken with modern photoelectric equipment. But this would not seem applicable over a large number of areas since one could not make simultaneous observations in all of the areas under study. While some errors are inherent in the photographs and in the measurement of densities on the photographs, a carefully planned photographic program seems to offer the best approach to the problem of further improvements in the photometric function.

SECTION XII

ACKNOWLEDGEMENTS

This work was supported by the National Aeronautics and Space Administration under NASA Grant No. NsG 468.

The authors are indebted to Dr. Laurence W. Frederick and the Leander McCormick Observatory for assistance, cooperation, and working space.

REFERENCES

[1] Fedoretz, V. A., "Photographic Photometry of the Lunar Surface," Publications of the Astronomical Observatory, Kharkov, Vol. 2, 1952.

[2] Sytinskaya, N. N. and Sharonov, V. V., "Investigation of the Reflectivity of the Lunar Surface." Publications of the Astronomical Observatory, Leningrad, Vol. 16, 114, 1952.

[3] Bennett, Arthur, L., "A Photovisual Investigation of the Brightness of 59 Areas on the Moon," Astrophysical Journal, Vol. 88, 1, 1938.

[4] Fessenkov, Parenago and Stoude, Publications of the Astronomical Institute of Russia, Vol. 4, 1, 1928.

[5] Opik, E., "Photometric Measures on the Moon and the Earth Shine," Publications of the Astronomical Observatory of the University of Tartu, Vol. 26, No. 1, 1924.

[6] Rougier, G., Annals of Strasbourg Observatory, Vol. 2 205, 1933.

[7] Herriman, Washburn and Willingham, "Ranger Preflight Science Analysis and the Lunar Photometric Model," Technical Report No. 32-384 (Rer.) Jet Propulsion Laboratory, Pasadena, California

[8] Van Diggelen, J., "Photometric Properties of Lunar Crater Floors," Recherches astronomique de l'observatoire d'Utrecht, The Netherlands, Vol. XIV, No. 2, 1959.

[9] Hopke, Bruce W., "A Theoretical Photometric Function for the Lunar Surface," Cornell University Center for Radiophysics and Space Research, Report No. 138, 1963.

[10] Sytinskaya, N. N., "Compound Catalog of Absolute Values of Visual Reflectivity of 104 Lunar Objects," Astronomical Journal of USSR, Vol. 30, 295, 1953.

[11] Fielder, G., "Structure of the Moon's Surface," Pergamon Press, London, 1961.

[12] Van Diggelen, "A Photometric Investigation of the Slopes at the Heights of the Ranges of Hills in the Maria of the Moon, "Bulletin of the Astronomical Institute of Netherlands, Vol. XI, p. 283, 1951.

[13] Minnoert, M., "The Reciprocity Principle in Lunar Photometry," Astrophysical Journal, Vol. 93, 403, 1941.

APPENDIX
THE PHOTOMETRIC FUNCTION; ϕ, PLOTTED AGAINST THE BRIGHTNESS LONGITUDE, α

On the following pages we show graphically the photometric function versus brightness longitude for numerous phases. The first 21 figures are based on the data of Fedoretz while the remaining ones are based on the data of Sytinskaya and Sharonov. The curves were fitted to the data by eye since no theoretical function seemed appropriate. On most of the curves a value of μ, the root mean square deviation from the hand curves, is shown. In the case of the data for $g = +4.^{\circ}5$, two straight lines have been drawn. The values of μ are similar for both. This emphasizes the bad scatter in these points.*

The values of ϕ were obtained as described above and assuming that for the available phase nearest zero, the value of ϕ was one.

Again as mentioned earlier, the brightness longitude, α, with respect to the brightness equator of the data of the photograph was calculated on the Burroughs 205 Computer. The inputs for this computer program included the spherical selenographic coordinates of all the required points and the coordinates of the sub-earth and sub-sun points for the date and hour at which each observation was actually made. These latter figures were obtained from the positions of the sun and Moon with respect to the earth as tabulated in the Nautical Almanac for the given dates.

---

* In each figure the point on the abcissa marked with a cross indicates the position of the terminator. The other form of the photometric function is obtained by plotting ϕ as a function of g with α as the parameter.

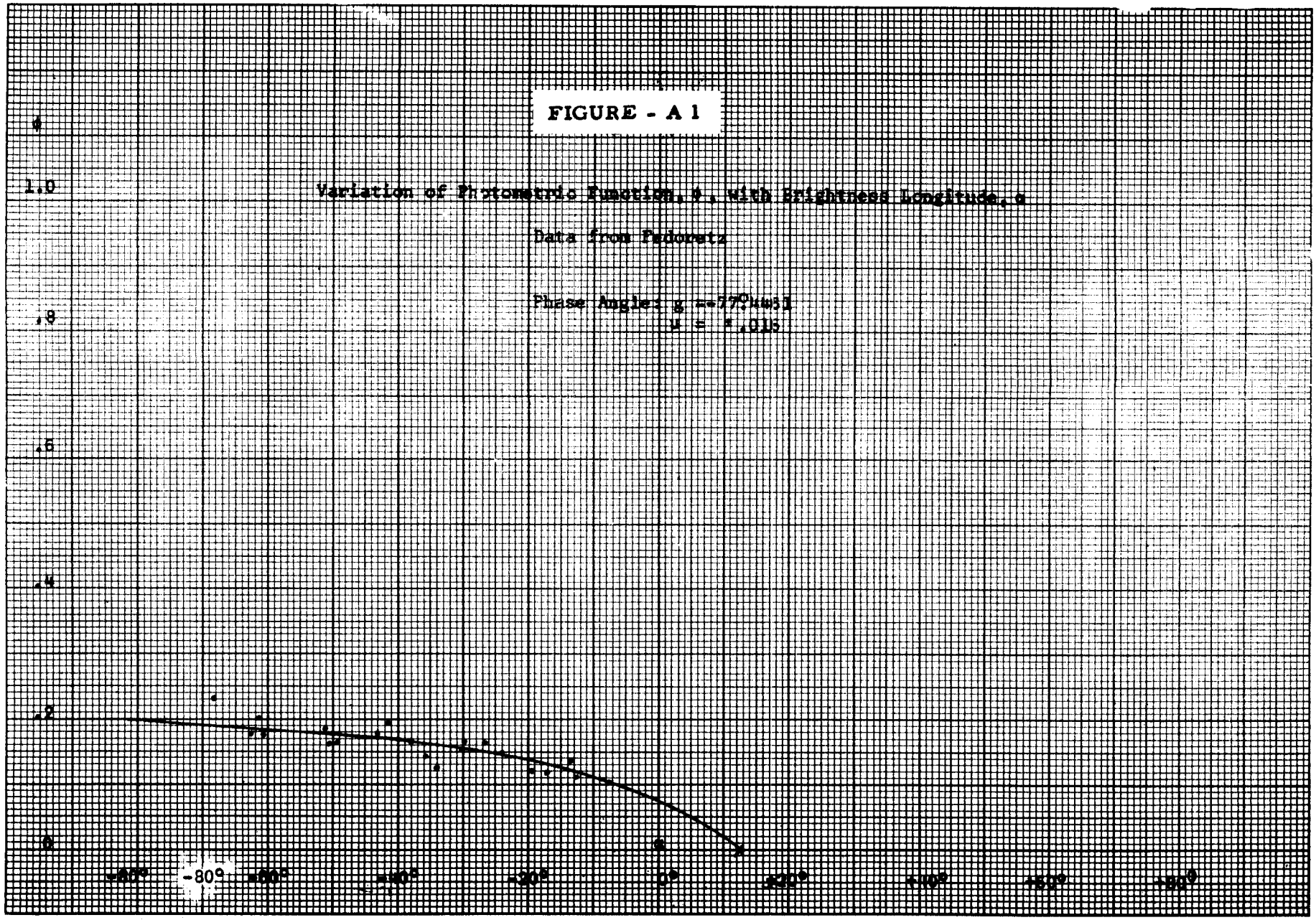
FIGURE - A 1
Variation of Photometric Function, Φ, with Brightness Longitude, α
Data from Fedoretz
Phase Angle: g = -77°.4 ± 0°.1
μ = ± .015
Φ
1.0
.8
.6
.4
.2
0
-80°
-60°
-40°
-20°
0°
+20°
+40°
+60°
+80°

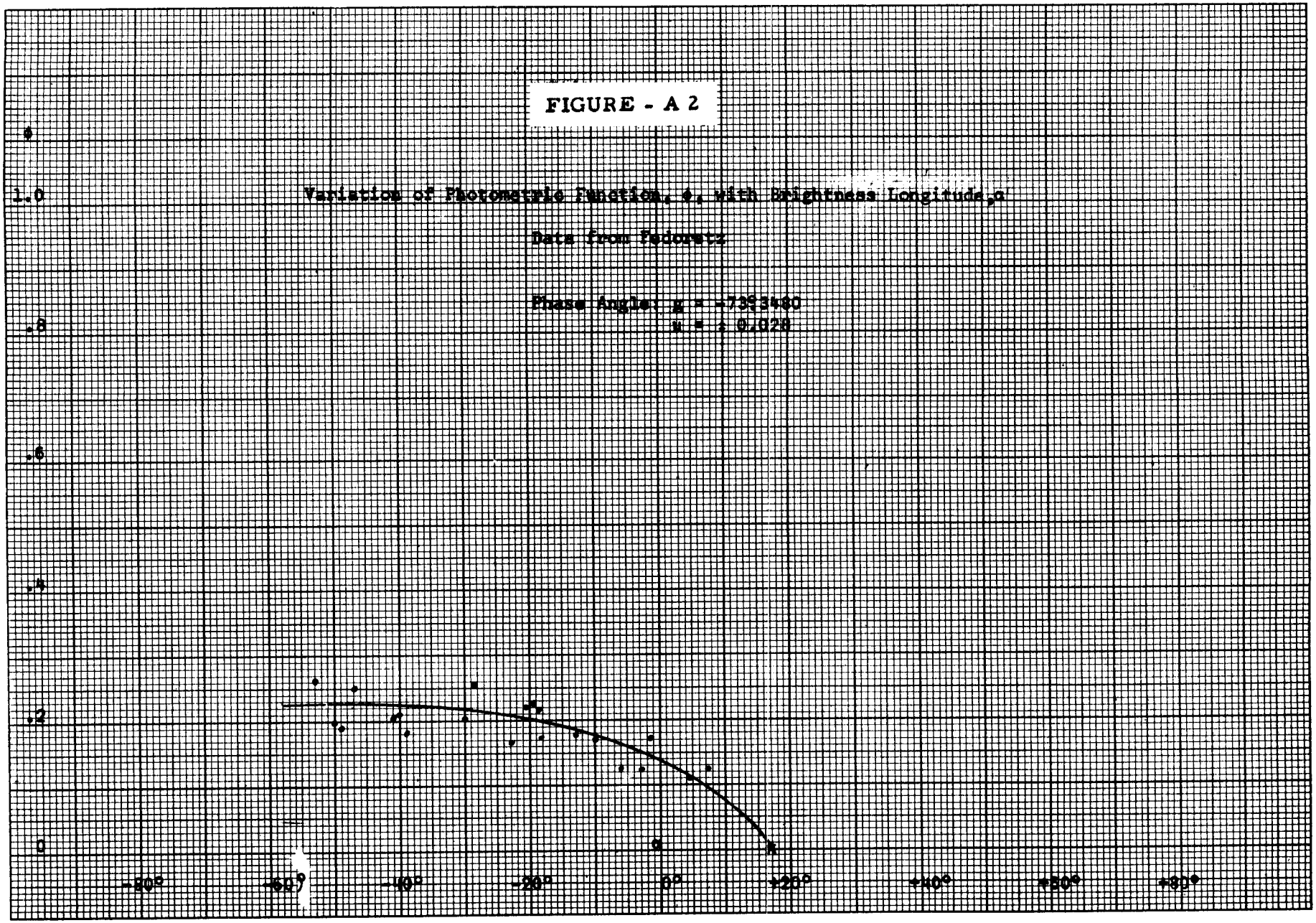
FIGURE - A 2
Variation of Photometric Function, Φ_1 with Brightness Longitude, a
Data from Fedorets
Phase Angle: g = -73°.3±.30
M = ± 0.028
Φ
1.0
.8
.6
.4
.2
0
-80°
-60°
-40°
-20°
0°
+20°
+40°
+60°
+80°

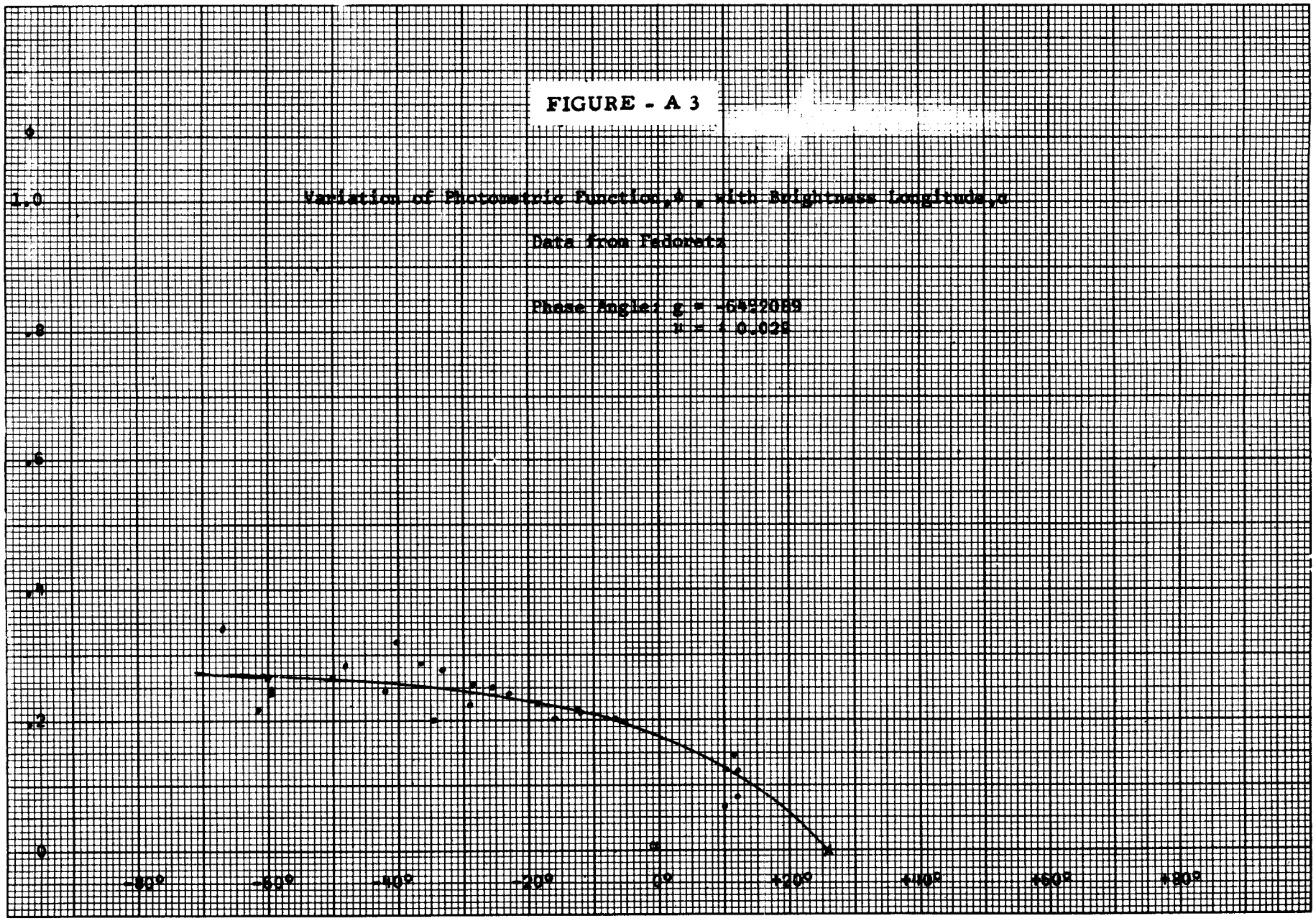
FIGURE - A 3
Variation of Photometric Function, Φ , with Brightness Longitude, α
Data from Fedorets
Phase Angle: g = -64°22'89
π = 1 0.02
1.0
.8
.6
.4
.2
0
-80°
-60°
-40°
-20°
0°
+20°
+40°
+60°
+80°

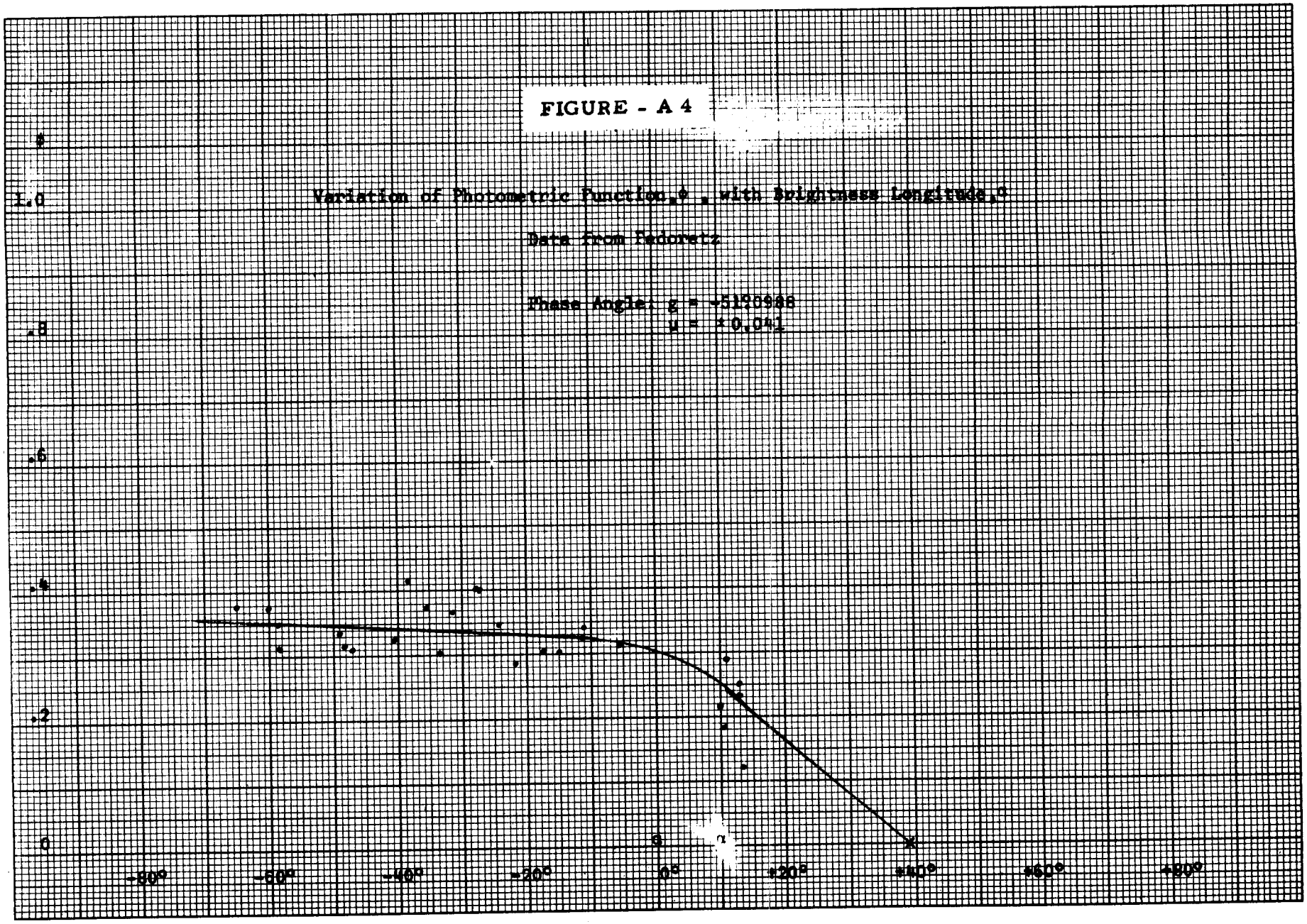
FIGURE - A 4
Variation of Photometric Function, Φ , with Brightness Longitude, Ω
Data from Fedoretz
Phase Angle: g = +51°.0988
μ = +0.041
Φ
1.0
.8
.6
.4
.2
0
-80°
-60°
-40°
-20°
0°
+20°
+40°
+60°
+80°
Ω

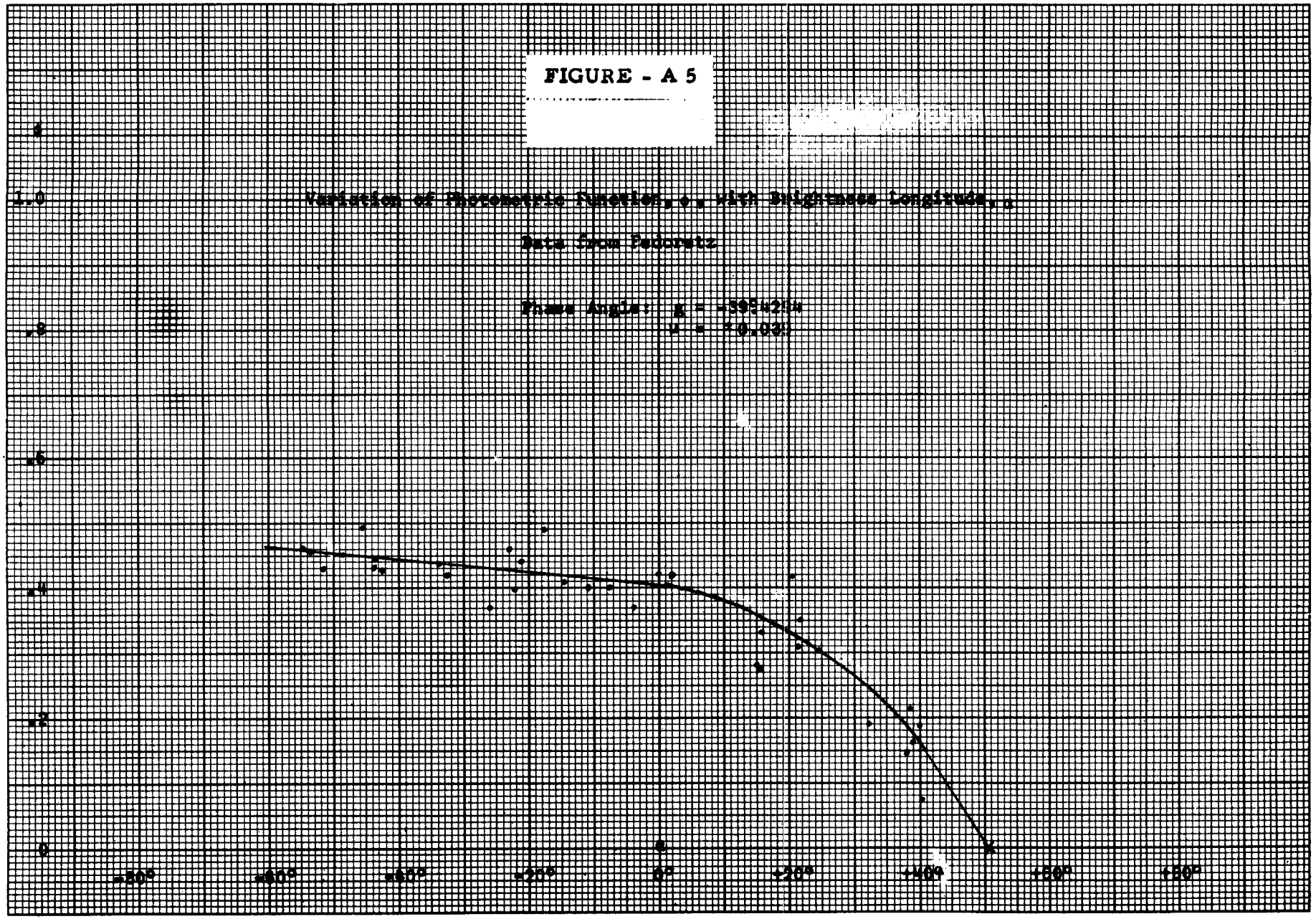
FIGURE - A 5
Variation of Photometric Function, ϕ_s with Brightness Longitude, α
Data from Pedoretz
Phase Angle: β = +39°42'.4
α = ±0.02'
1.0
.8
.6
.4
.2
0
-80°
-60°
-40°
-20°
0°
+20°
+40°
+60°
+80°

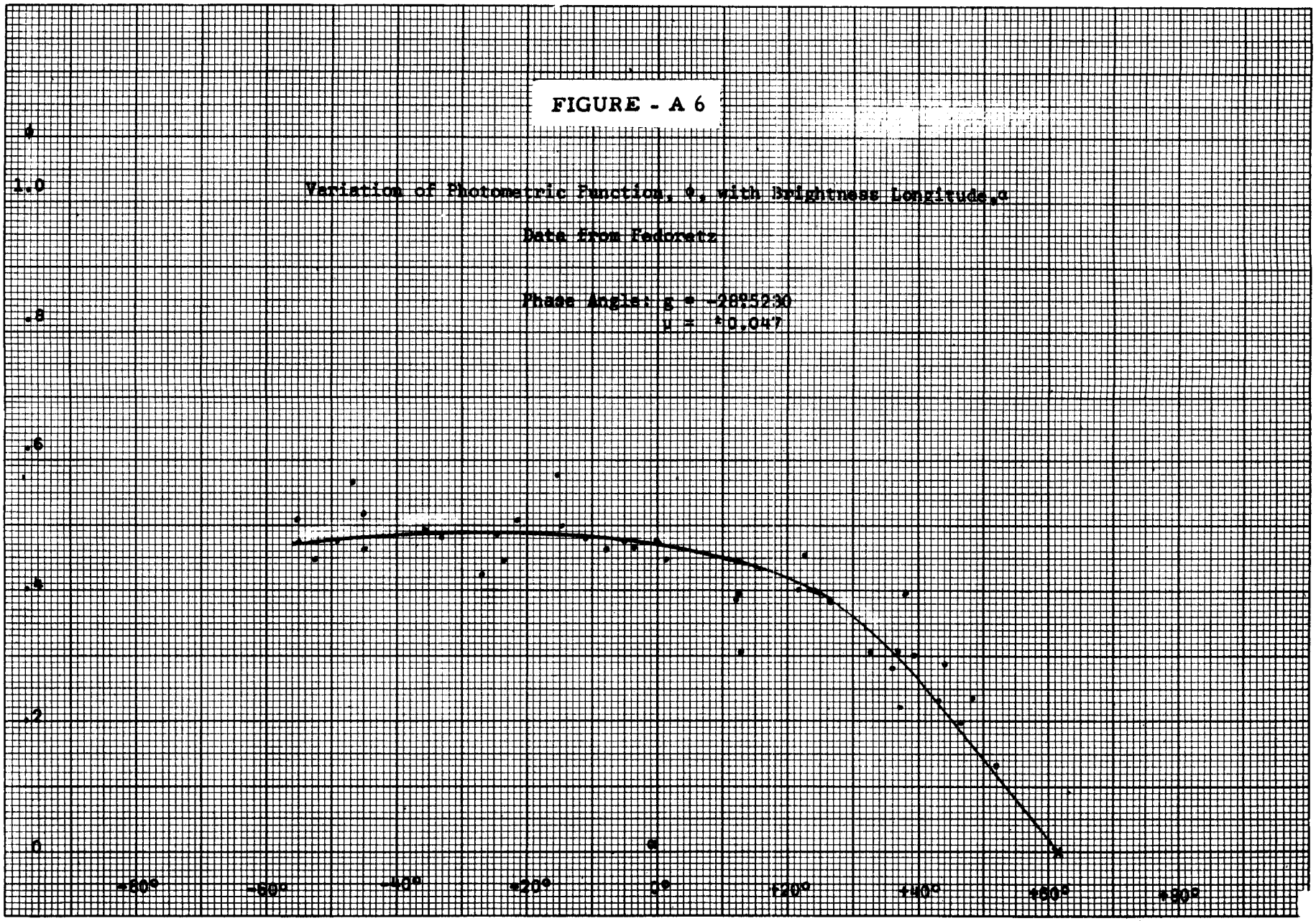
FIGURE - A 6
Variation of Photometric Function, Φ, with Brightness Longitude, α
Data from Fedoretz
Phase Angle: g = -28°52'30"
μ = ±0,047
Φ
1.0
.8
.6
.4
.2
0
α
-60°
-60°
-40°
-20°
0°
+20°
+40°
+60°
+80°

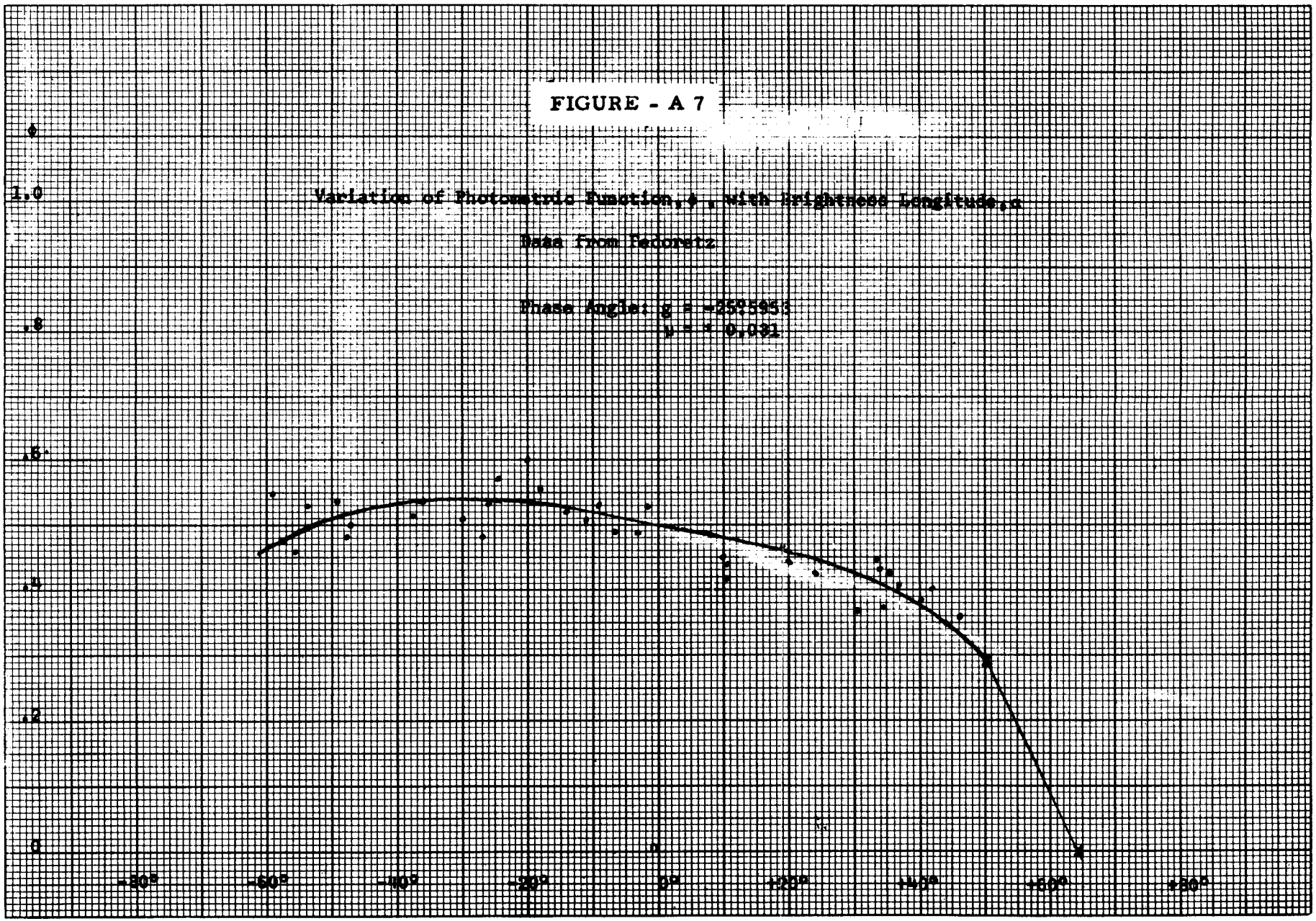
FIGURE - A 7
Variation of Photometric Function, Φ, with Brightness Longitude, α
Data from Fedorets
Phase Angle: g = -25°.5953
ψ = + 0,031
Φ
1,0
,8
,6
,4
,2
0
-80°
-60°
-40°
-20°
0°
+20°
+40°
+60°
+80°

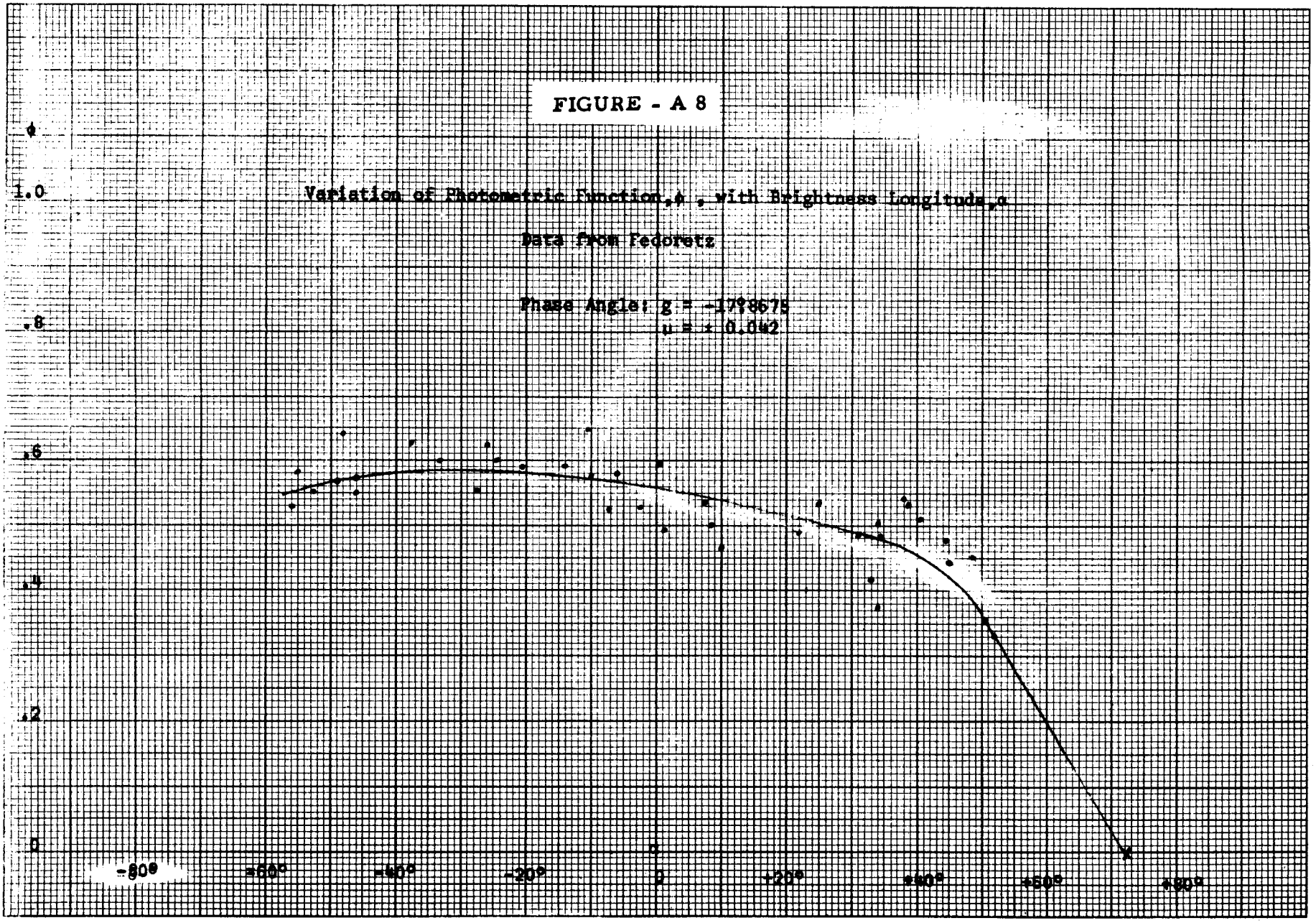
FIGURE - A 8
Variation of Photometric Function, Φ , with Brightness Longitude, α
Data from Fedoretz
Phase Angle: g = -1°.98675
μ = ± 0.042
Φ
1.0
.8
.6
.4
.2
0
-80°
-60°
-40°
-20°
0
+20°
+40°
+60°
+80°

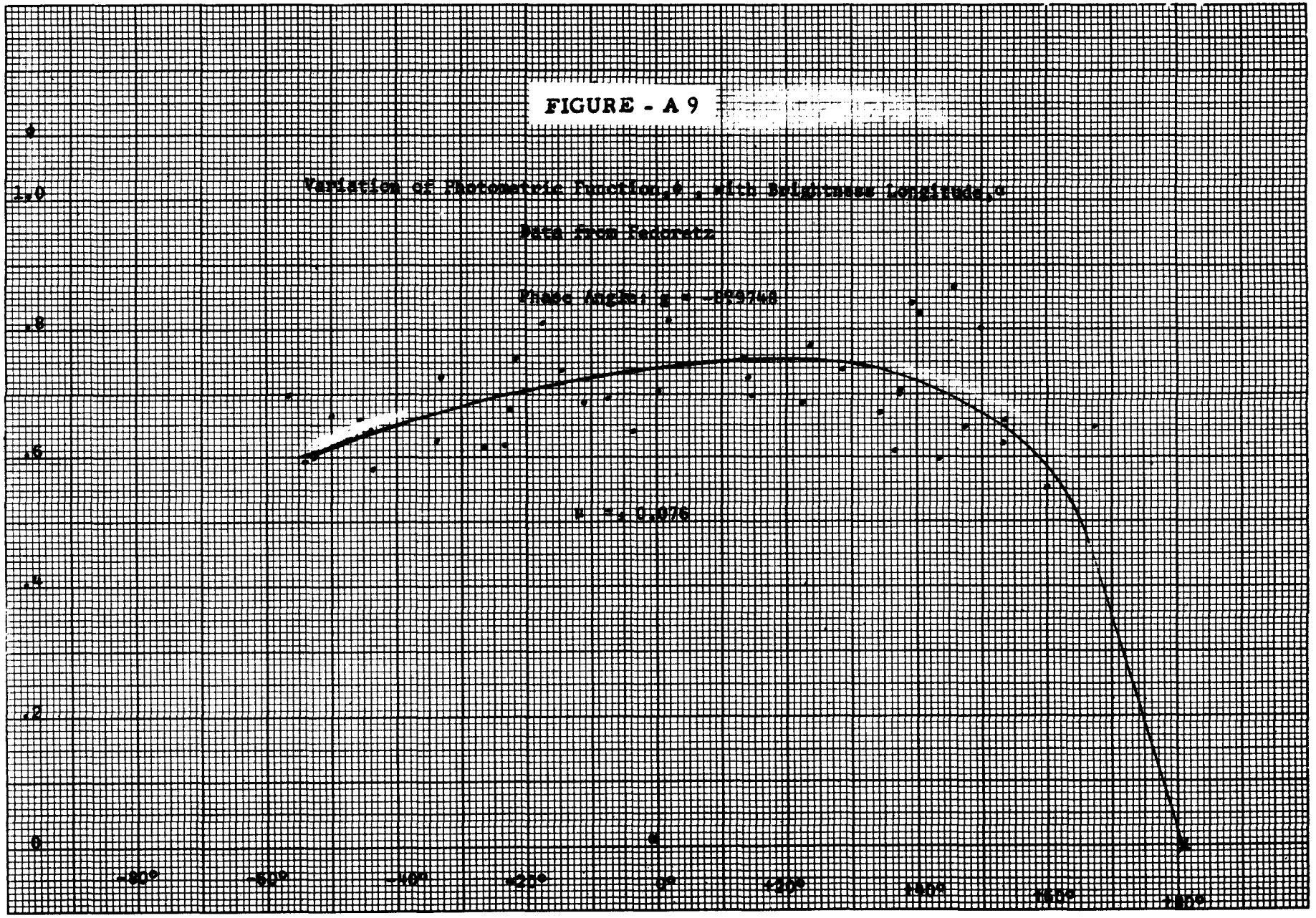
FIGURE - A 9
Variation of Photometric Function, Φ , with Selenocentric Longitude, ℓ
Data from Fedorets
Phase Angle: g = -0°39'48"
1.0
.8
.6
.4
.2
0
r = 0.076
-60°
-50°
-40°
-20°
0°
+20°
+40°
+60°
+80°

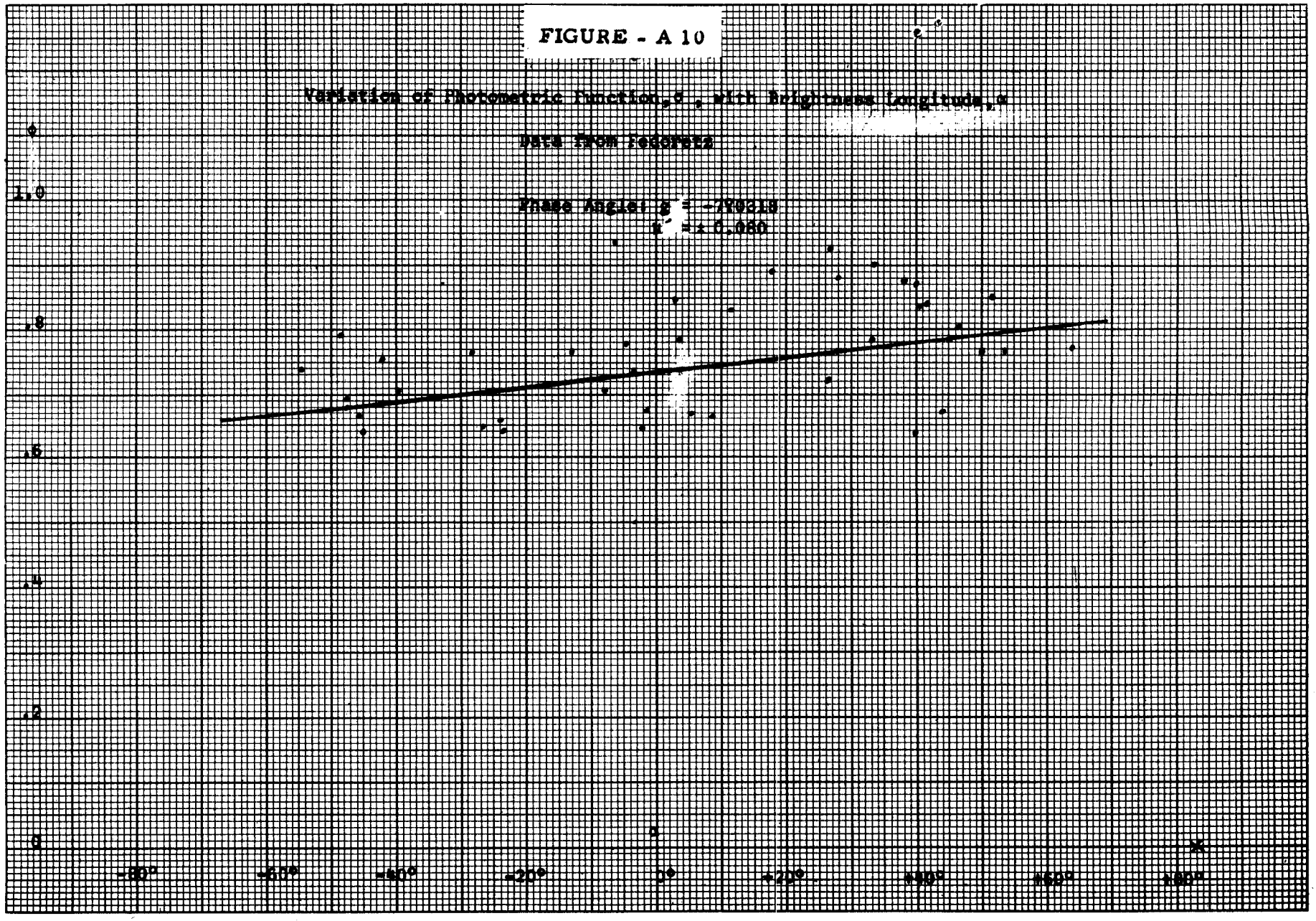
FIGURE - A 10
Variation of Photometric Function, Φ , with Brightness Longitude, ψ
Data from Fedorets
Phase Angle: β = -7°0319
σ = ± 0.080
1.0
.8
.6
.4
.2
0
-80°
-60°
-40°
-20°
0°
+20°
+40°
+60°
+80°

FIGURE - A 11

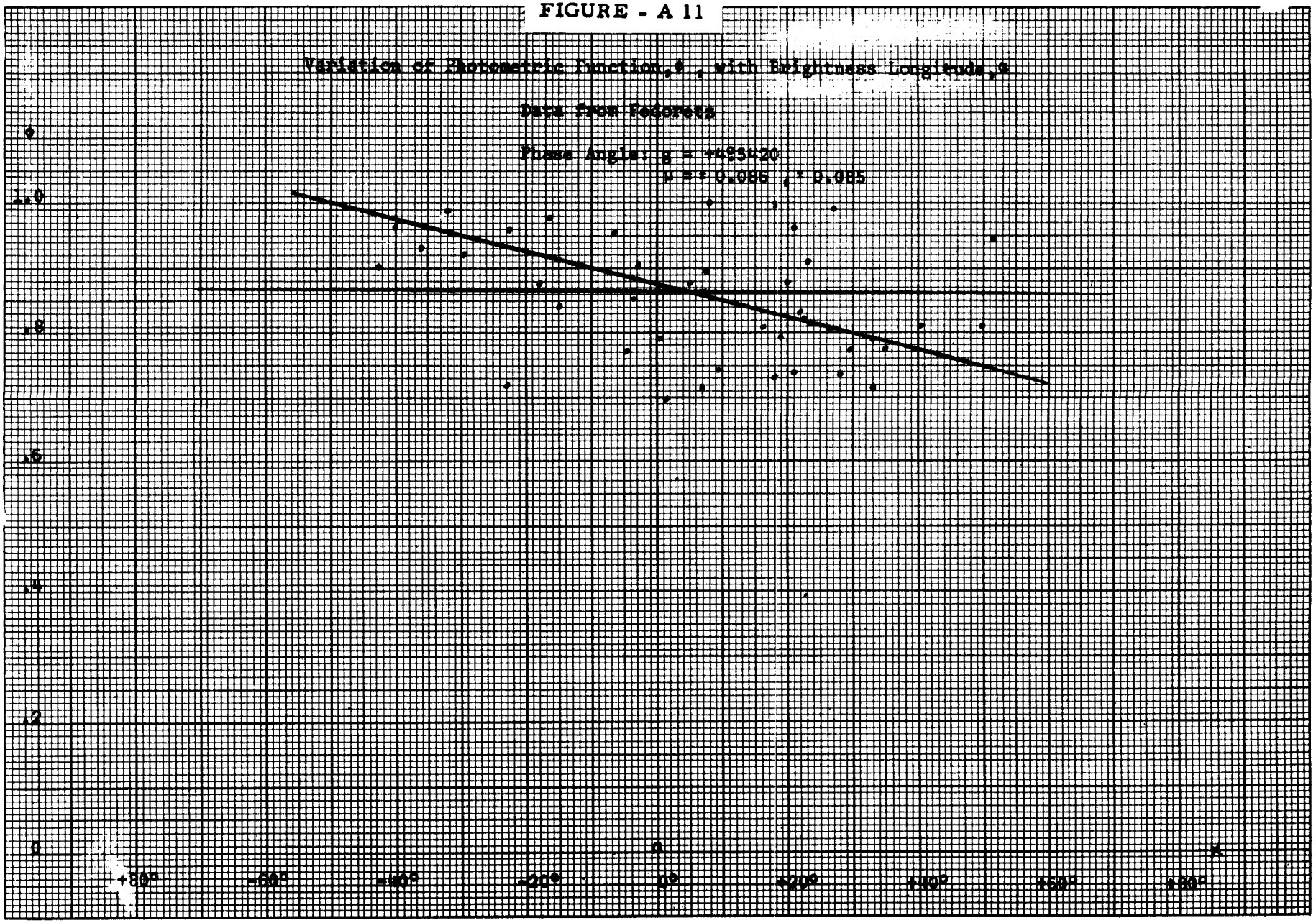
Variation of Photometric Function, Φ, with Brightness Longitude, Θ
Data from Fedoretz
Phase Angle: g = +4°34'20"
γ = ± 0.086 ; ± 0.085
1.0
.8
.6
.4
.2
0
+80°
-60°
-40°
-20°
0°
+20°
+40°
+60°
+80°

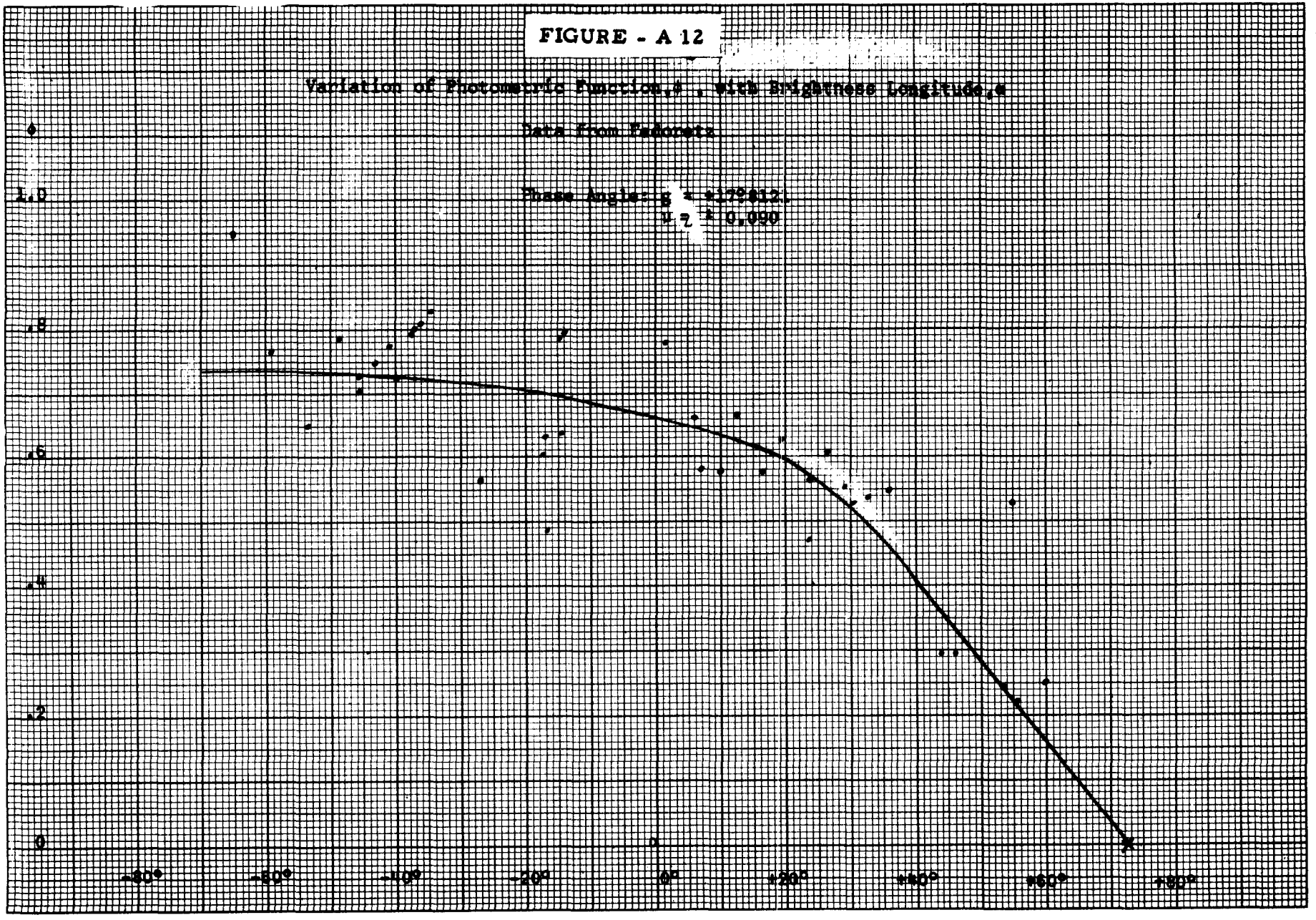
FIGURE - A 12
Variation of Photometric Function, Φ , with Brightness Longitude, ε
Data from Fedorets
Phase Angle: g = +179°12'.
μ z = 0.090
1.0
.8
.6
.4
.2
0
-80°
-60°
-40°
-20°
0°
+20°
+40°
+60°
+80°

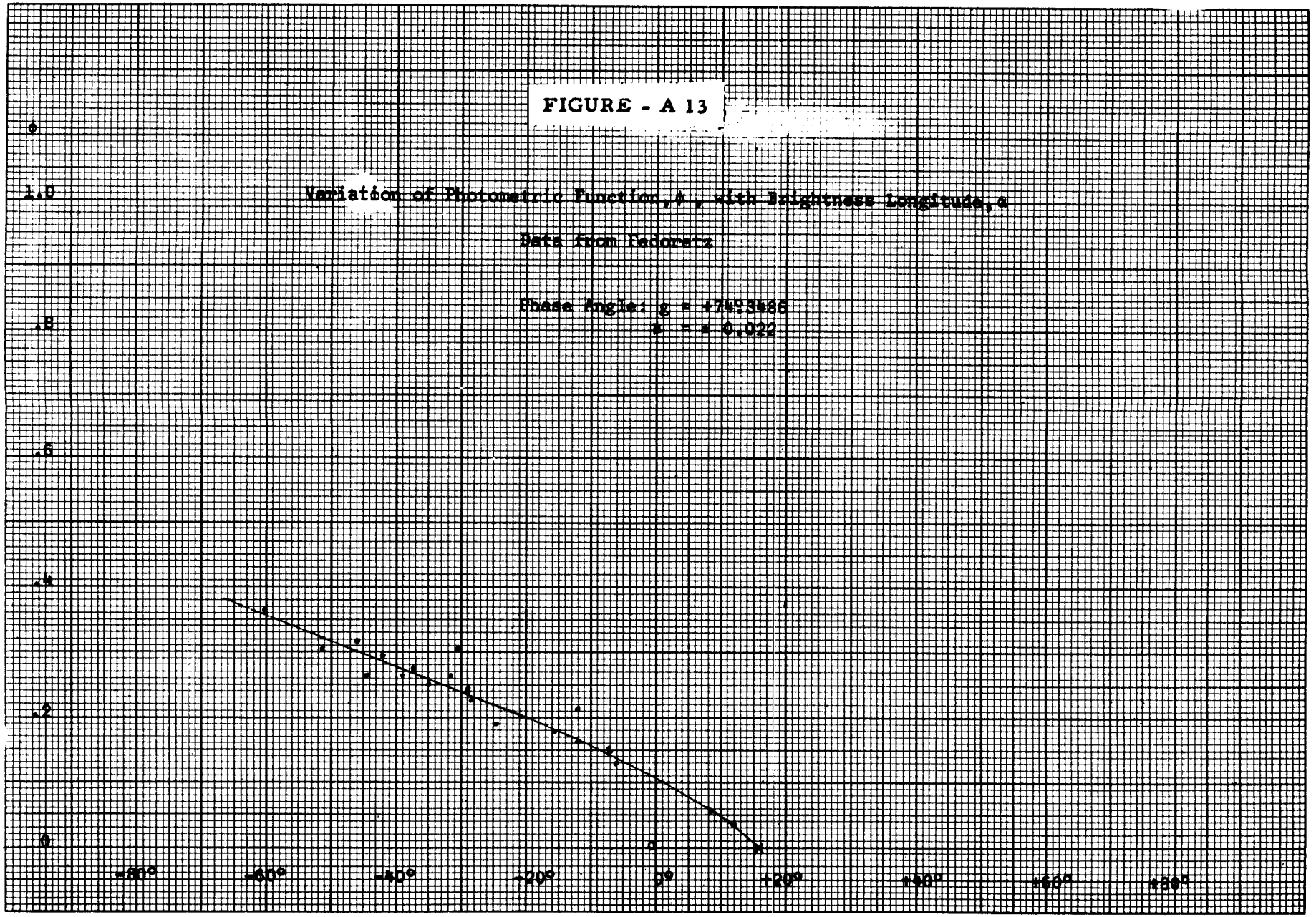
FIGURE - A 13
Variation of Photometric Function, Φ, with Brightness Longitude, α
Data from Fedorets
Phase Angle: g = +74°.3486
Φ = 0.022
Φ
1.0
.8
.6
.4
.2
0
-80°
-60°
-40°
-20°
0°
+20°
+40°
+60°
+80°

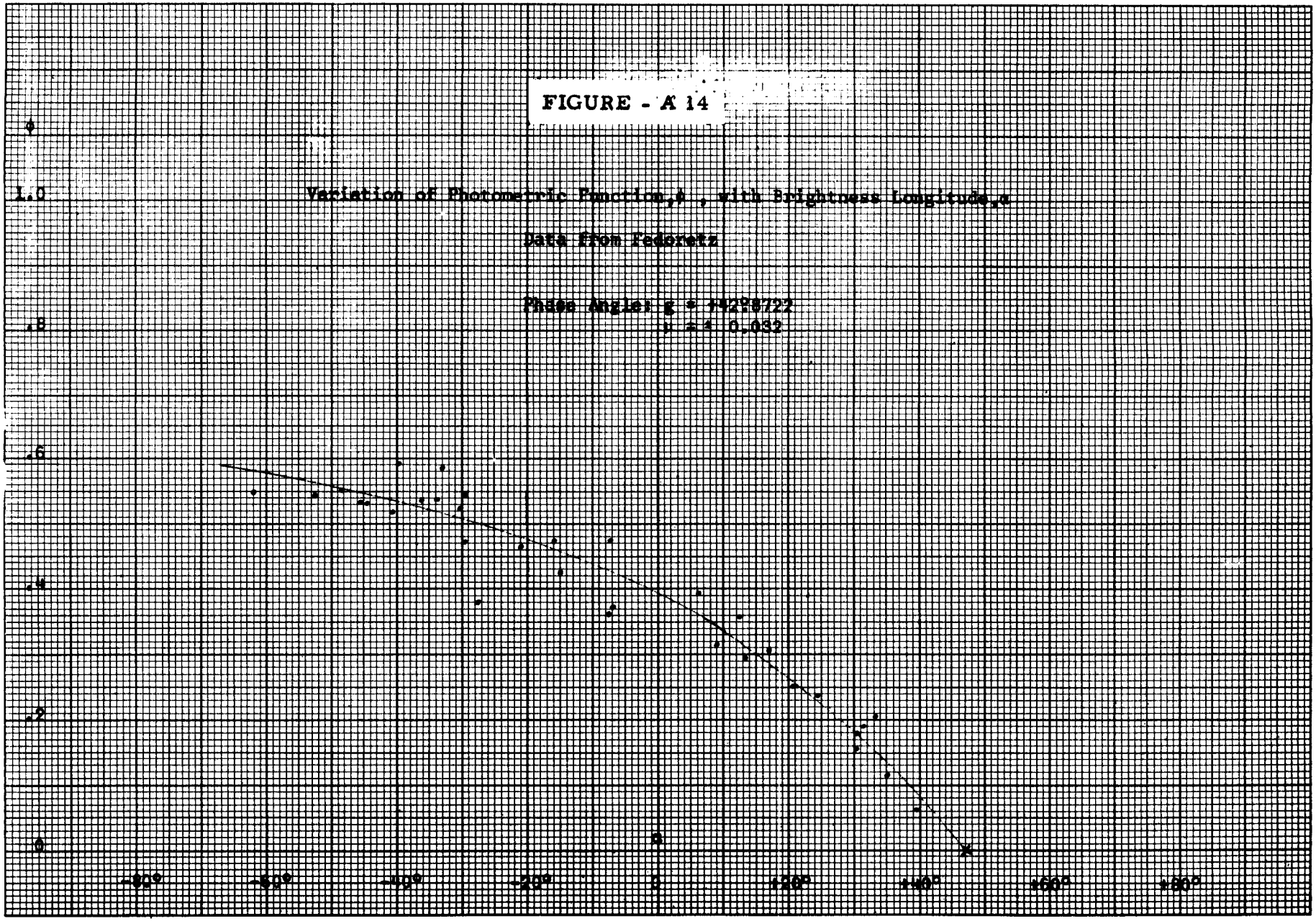
FIGURE - A 14
Variation of Photometric Function, Φ , with Brightness Longitude, α
Data from Fedoretz
Phase Angle: g = 1°42'.8722
μ = ± 0.032
Φ
1.0
.8
.6
.4
.2
0
-80°
-60°
-40°
-20°
0
+20°
+40°
+60°
+80°

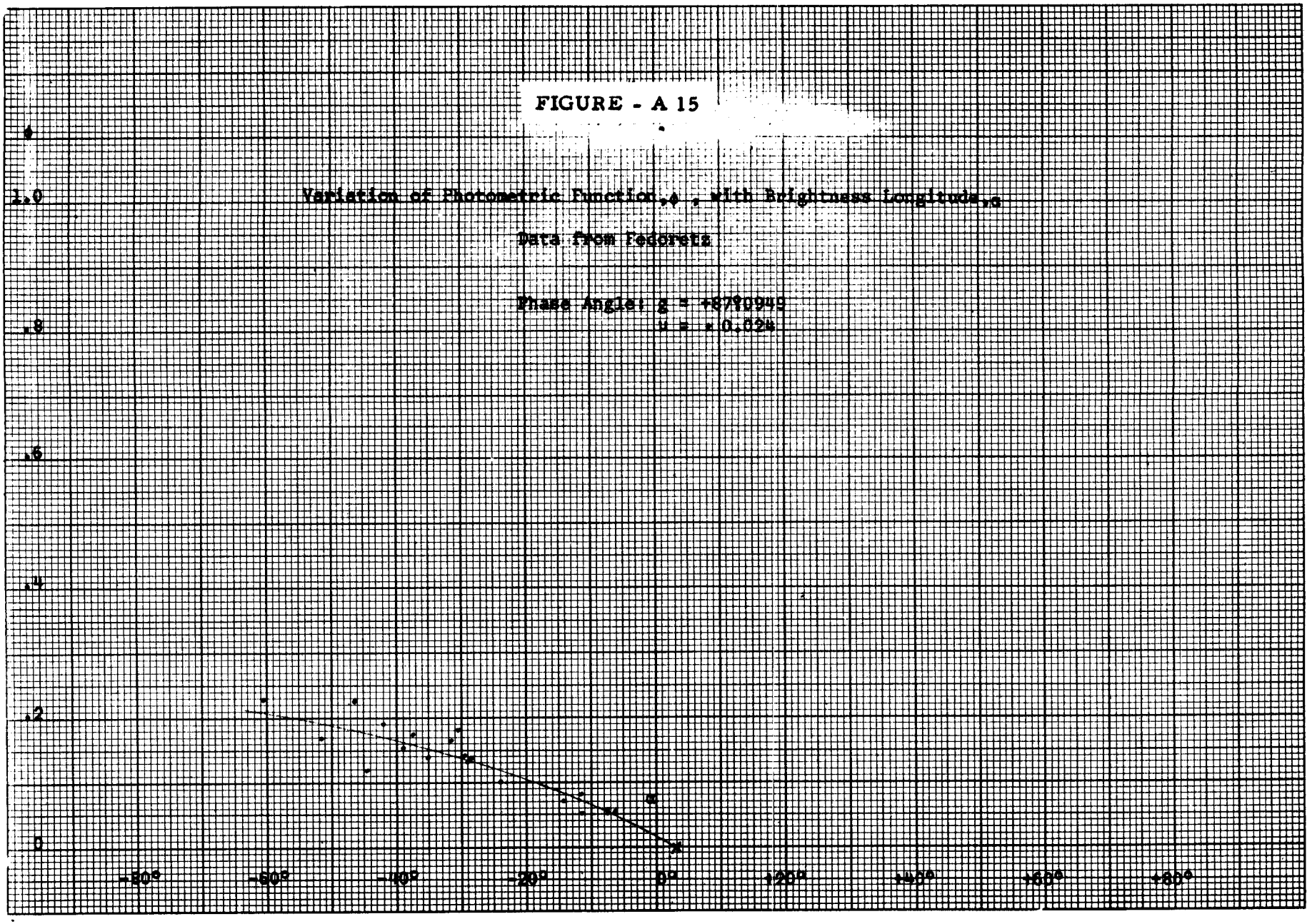
FIGURE - A 15
Variation of Photometric Function, Φ , with Brightness Longitude, G
Data from Fedorets
Phase Angle: g = +8°.0949
u = +0.824
Φ
1.0
.8
.6
.4
.2
0
-80°
-60°
-40°
-20°
0°
+20°
+40°
+60°
+80°

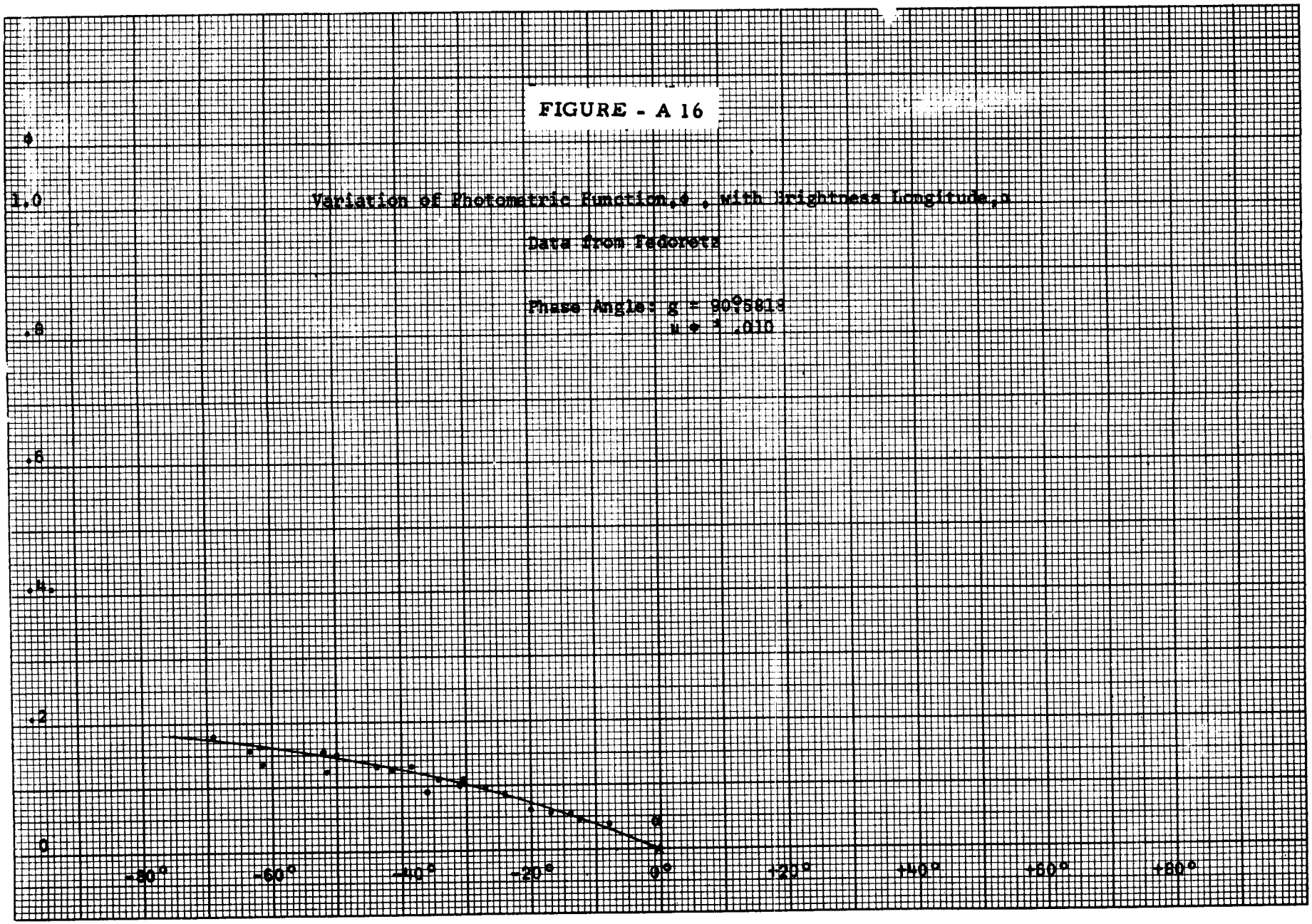
FIGURE - A 16
Variation of Photometric Function, Φ , with Brightness Longitude, a
Data from Fedorets
Phase Angle: g = 90°.5813
u Φ = .010
Φ
1.0
.8
.6
.4
.2
0
-80°
-60°
-40°
-20°
0°
+20°
+40°
+60°
+80°

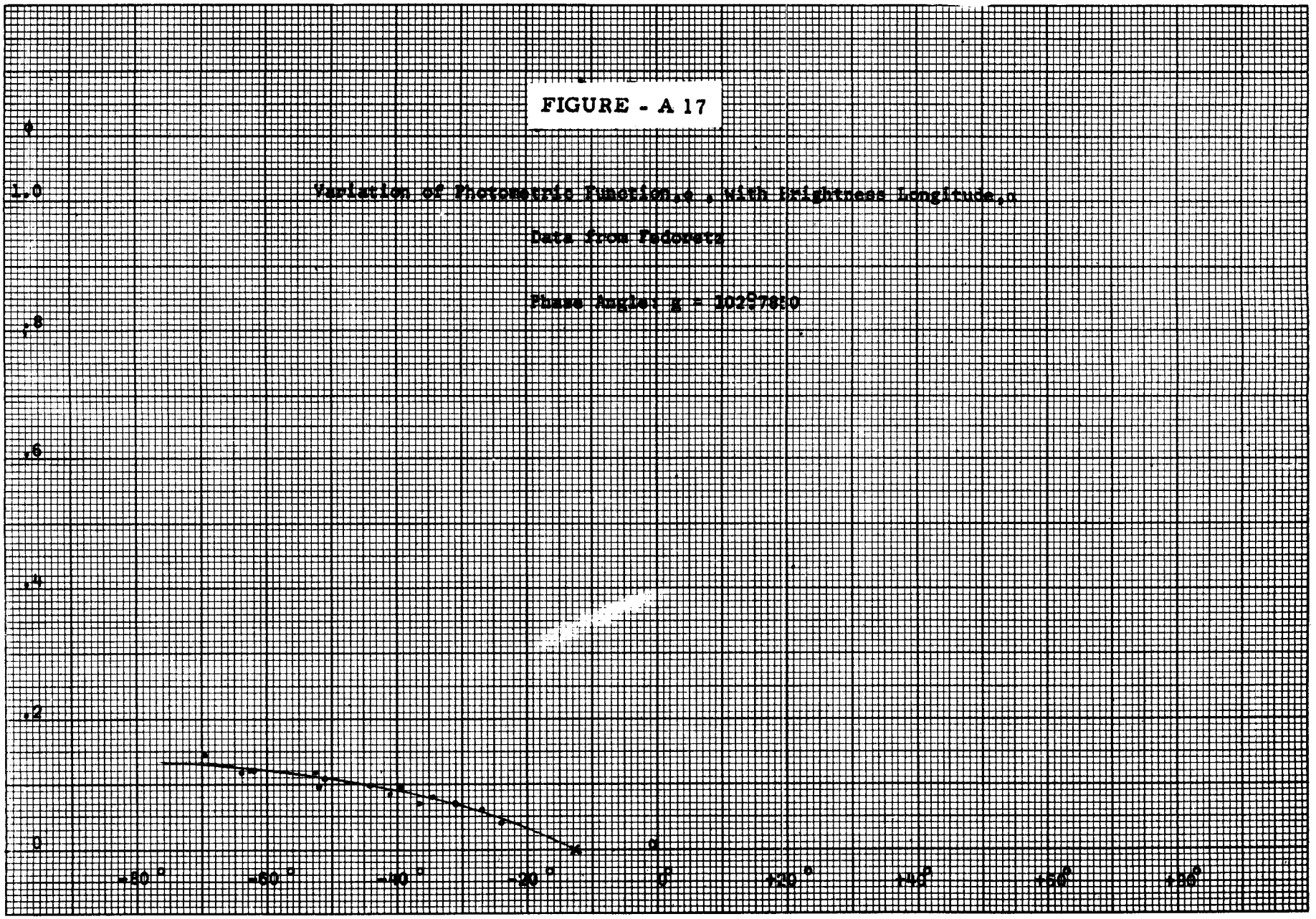
FIGURE - A 17
Variation of Photometric Function, φ , with Brightness Longitude, α
Data from Fedorets
Phase Angle: χ = 102°78:0
φ
1.0
.8
.6
.4
.2
0
-80°
-60°
-40°
-20°
0°
+20°
+40°
+60°
+80°

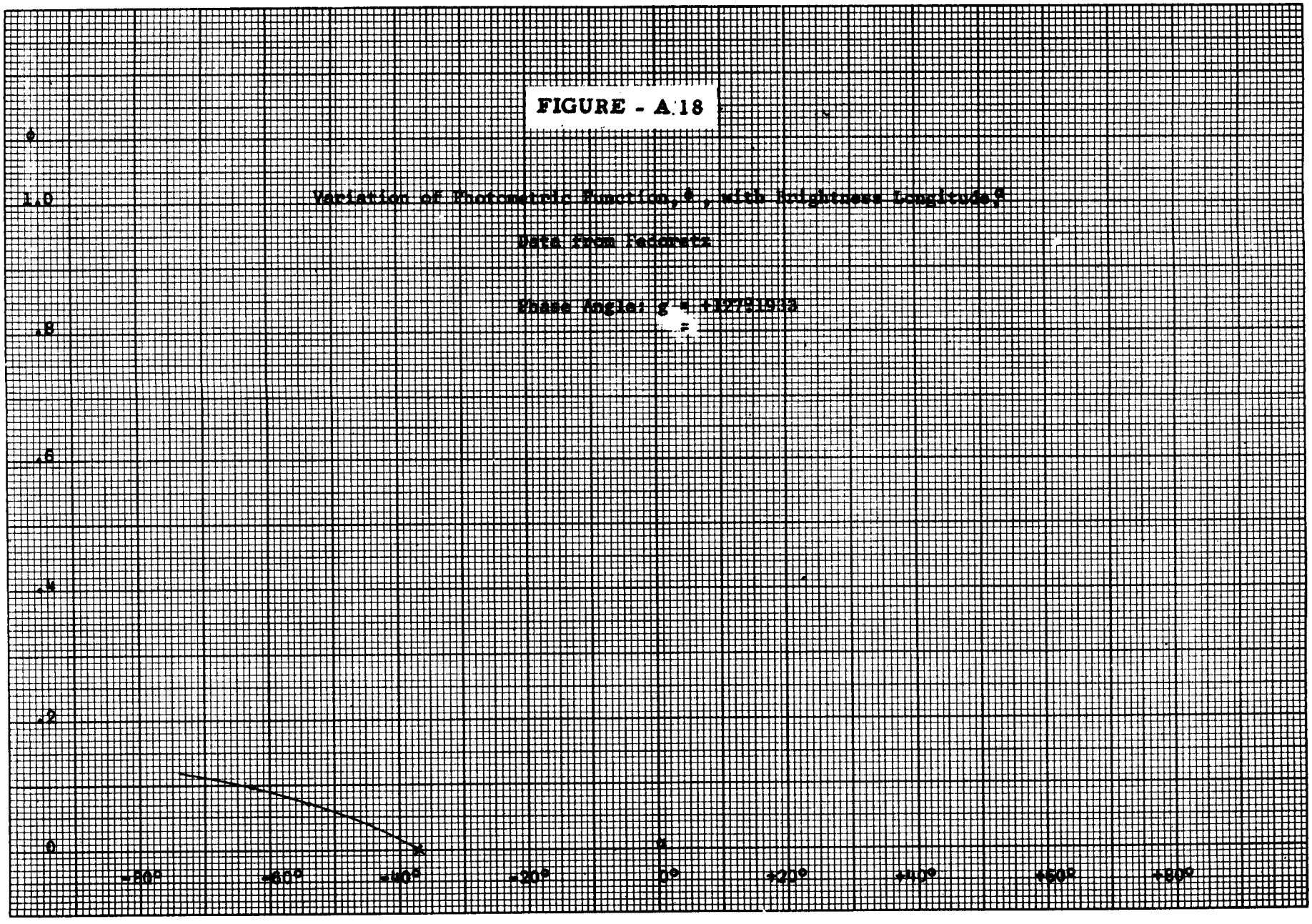
FIGURE - A 18
Variation of Photometric Function, Φ_y, with Brightness Longitude, β
Data from Radonetz
Phase Angle: g = +127°19'33
Φ
1.0
.8
.6
.4
.2
0
-80°
-60°
-40°
-20°
0°
+20°
+40°
+60°
+80°
β

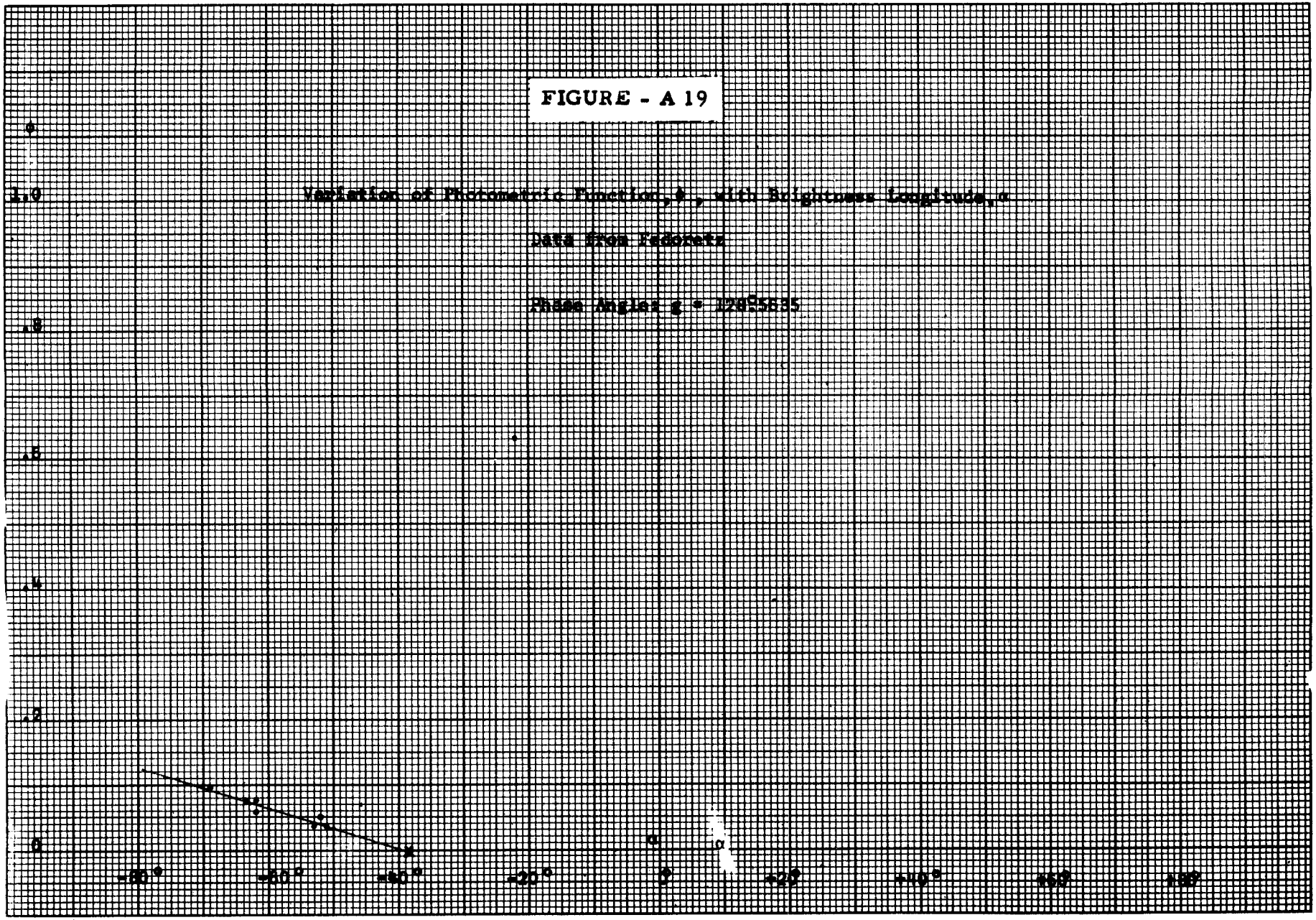
FIGURE - A 19
Variation of Photometric Function, Φ, with Brightness Longitude, α
Data from Fedoretz
Phase Angle: ε = 120°58'35"
1.0
.8
.6
.4
.2
0
-80°
-60°
-40°
-20°
0°
+20°
+40°
+60°
+80°

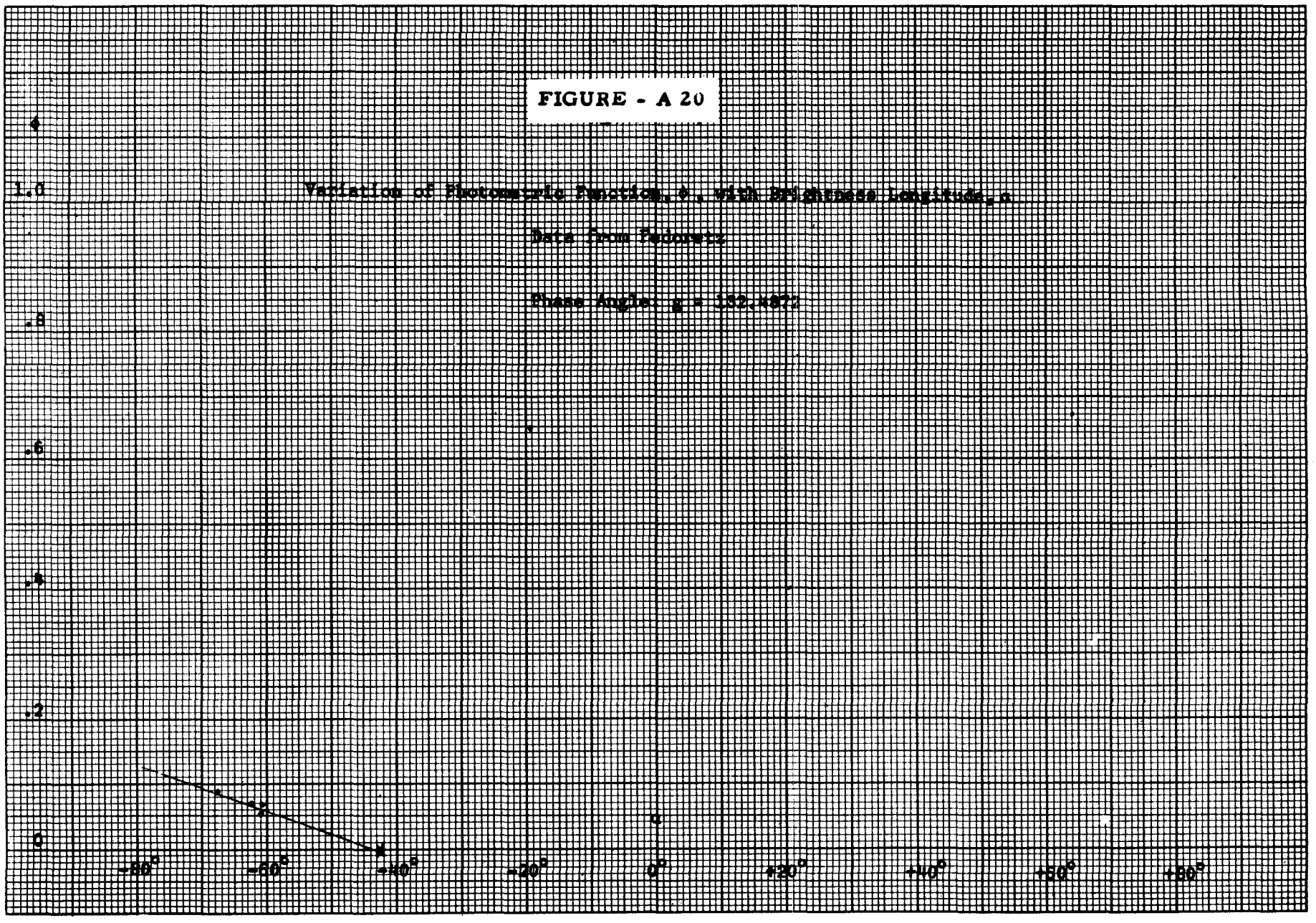
FIGURE - A 20
Variation of Photometric Function, Φ, with Brightness Longitude, α
Data from Fedorets
Phase Angle: β = 182.48°
1.0
.8
.6
.4
.2
0
-80°
-60°
-40°
-20°
0°
+20°
+40°
+60°
+80°

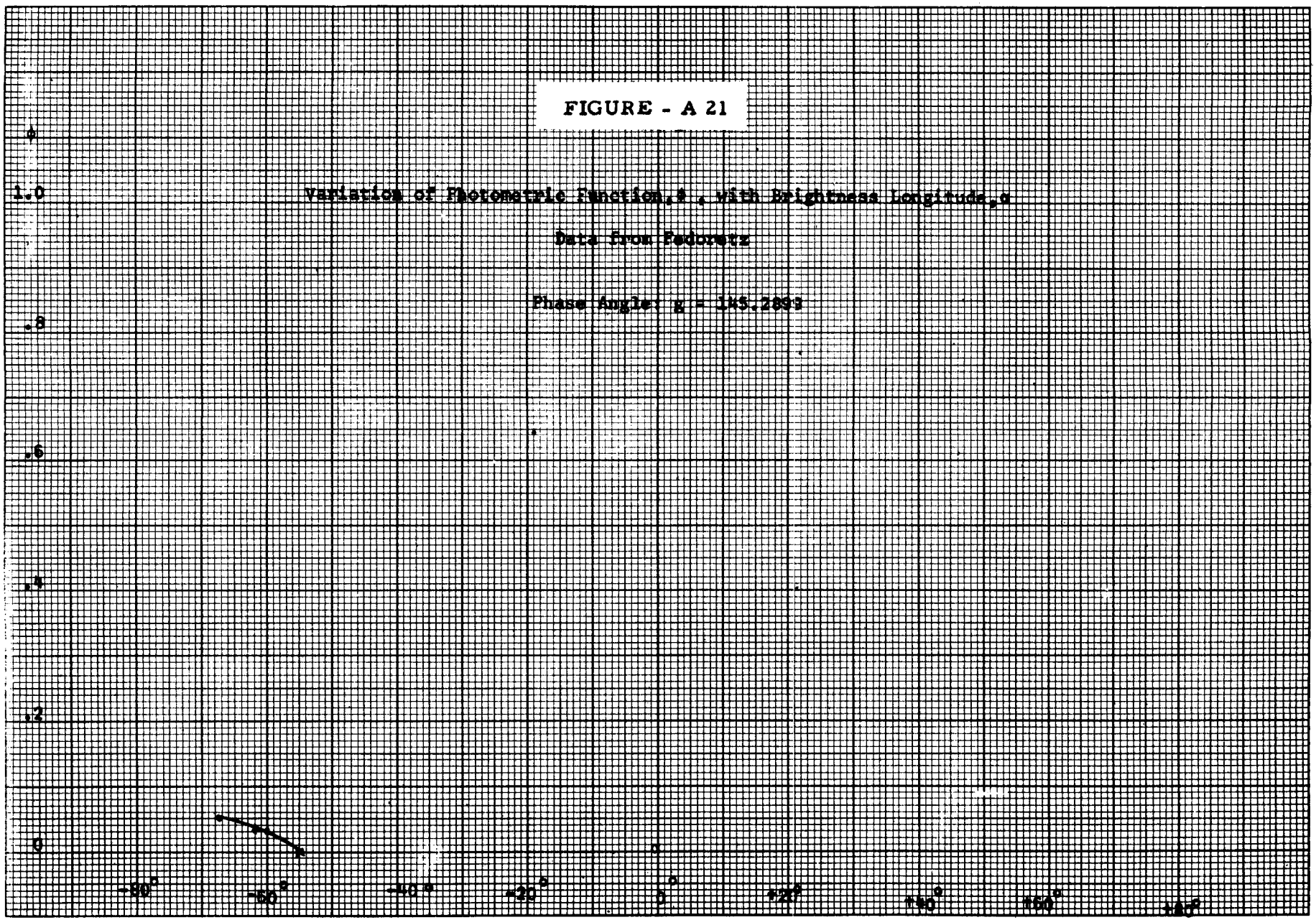
FIGURE - A 21
Variation of Photometric Function, Φ , with Brightness Longitude, σ
Data from Fedoretz
Phase Angle: α = 145.2893
Φ
1.0
.8
.6
.4
.2
0
-80°
-60°
-40°
-20°
0°
+20°
+40°
+60°
+80°

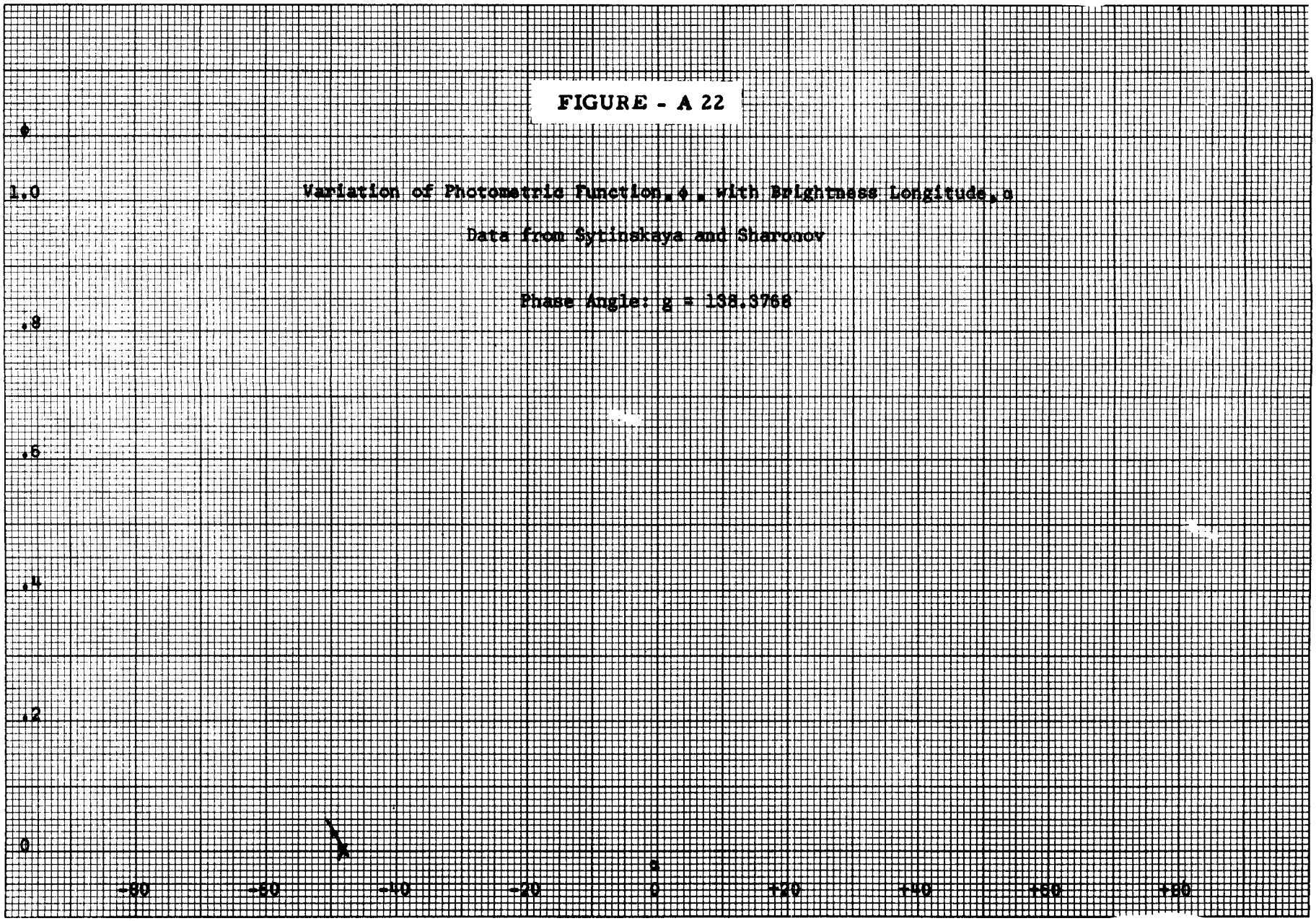
FIGURE - A 22
Variation of Photometric Function, Φ, with Brightness Longitude, a
Data from Sytinskaya and Sharonov
Phase Angle: g = 138.3768
Φ
1.0
.8
.6
.4
.2
0
-80
-60
-40
-20
0
+20
+40
+60
+80

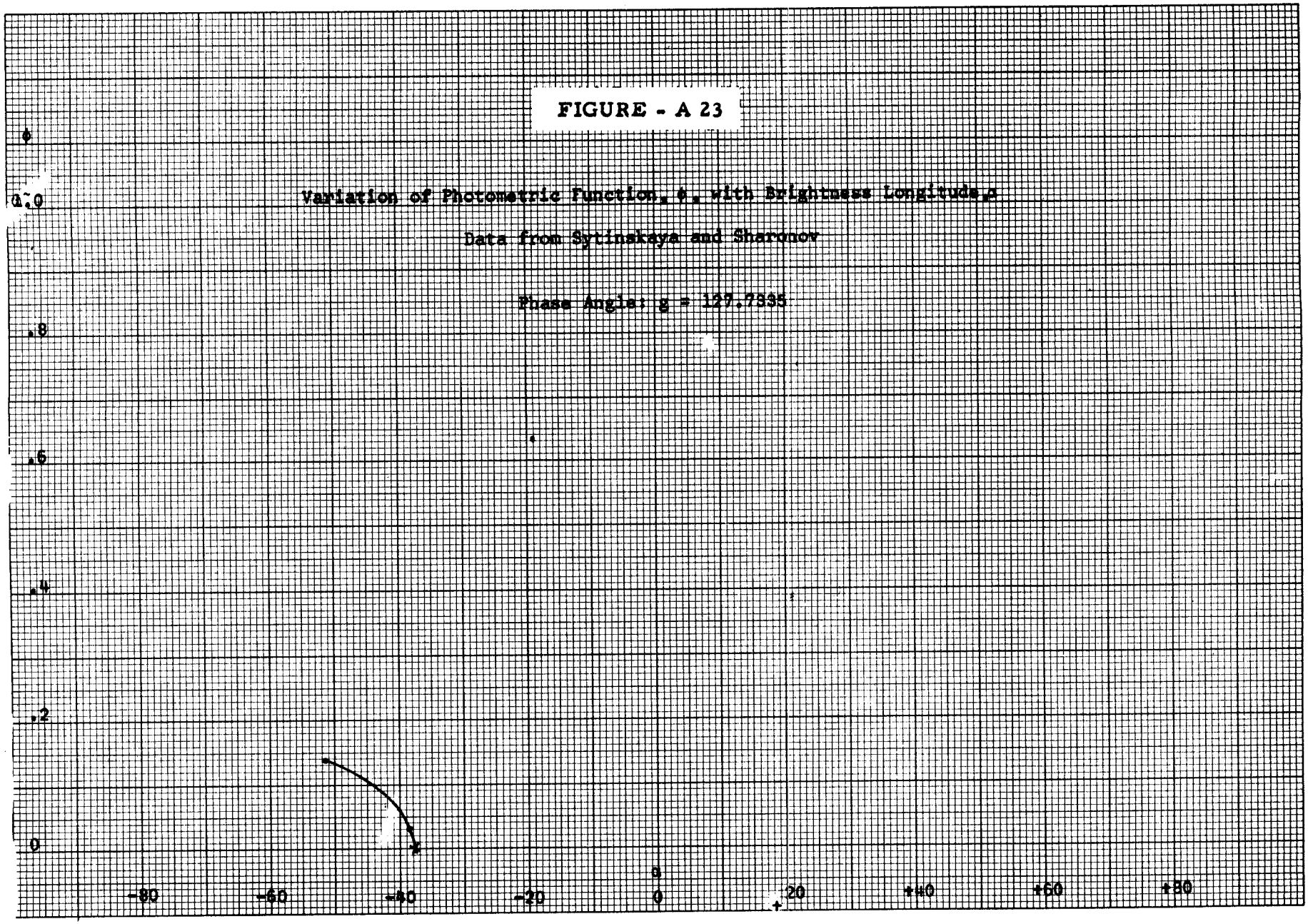
FIGURE - A 23
Variation of Photometric Function, ϕ, with Brightness Longitude, a
Data from Sytinskaya and Sharonov
Phase Angle: g = 127.7335
ϕ
1.0
.8
.6
.4
.2
0
-80
-60
-40
-20
0
+20
+40
+60
+80
a

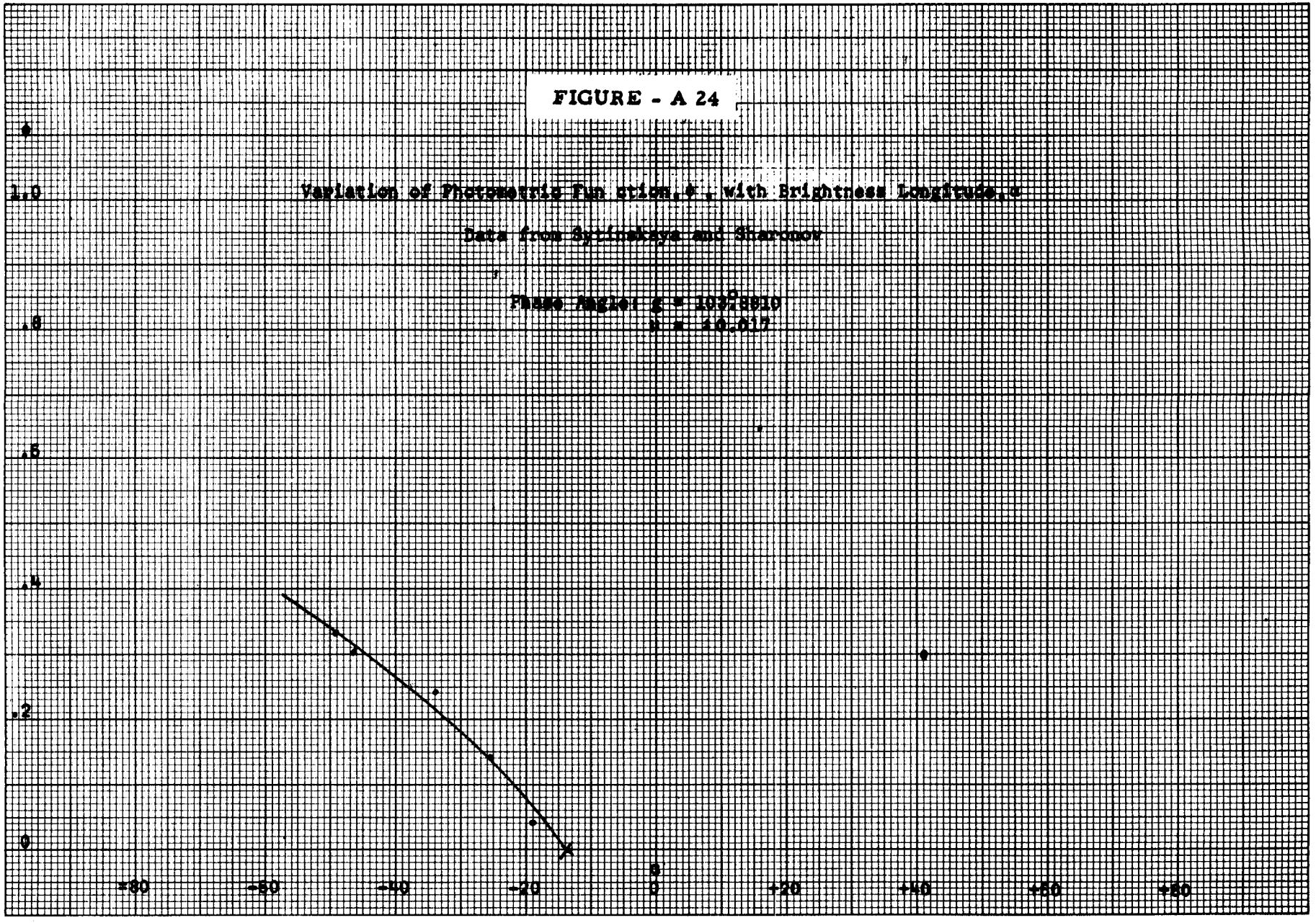
FIGURE - A 24
Variation of Photometric Fun ction, Φ , with Brightness Longitude, α
Data from Sytinskaya and Sharonov
Phase Angle: g = 103°.8810
a = 10.017
Φ
1.0
.8
.6
.4
.2
0
-80
-60
-40
-20
0
+20
+40
+60
+80
α
0

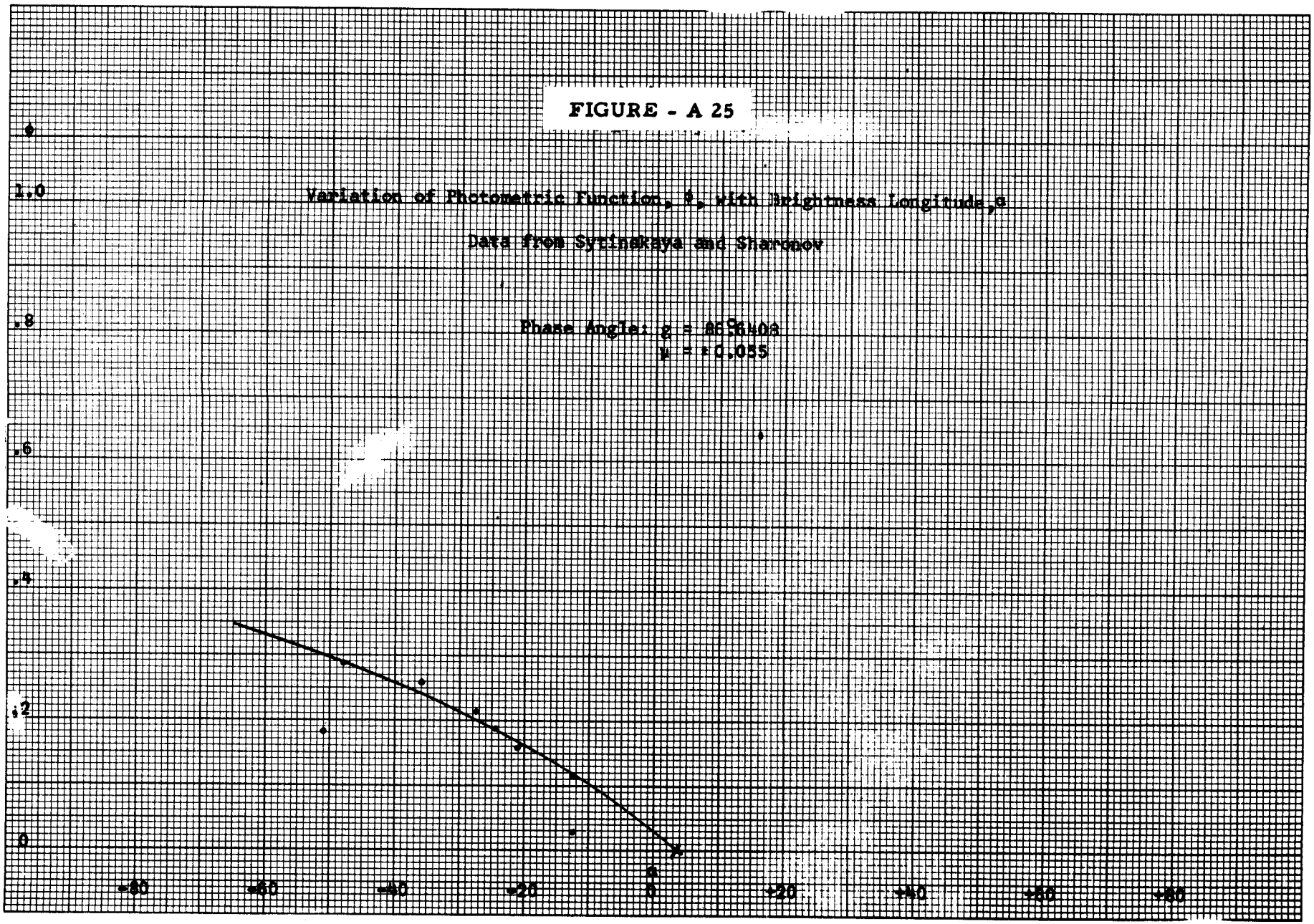
FIGURE - A 25
Variation of Photometric Function, Φ, with Brightness Longitude, θ
Data from Syrinskaya and Sharonov
Phase Angle: g = 86.96±03
ψ = ±0.055
Φ
1.0
.8
.6
.4
.2
0
-80
-60
-40
-20
0
+20
+40
+60
+80
θ

FIGURE - A 26

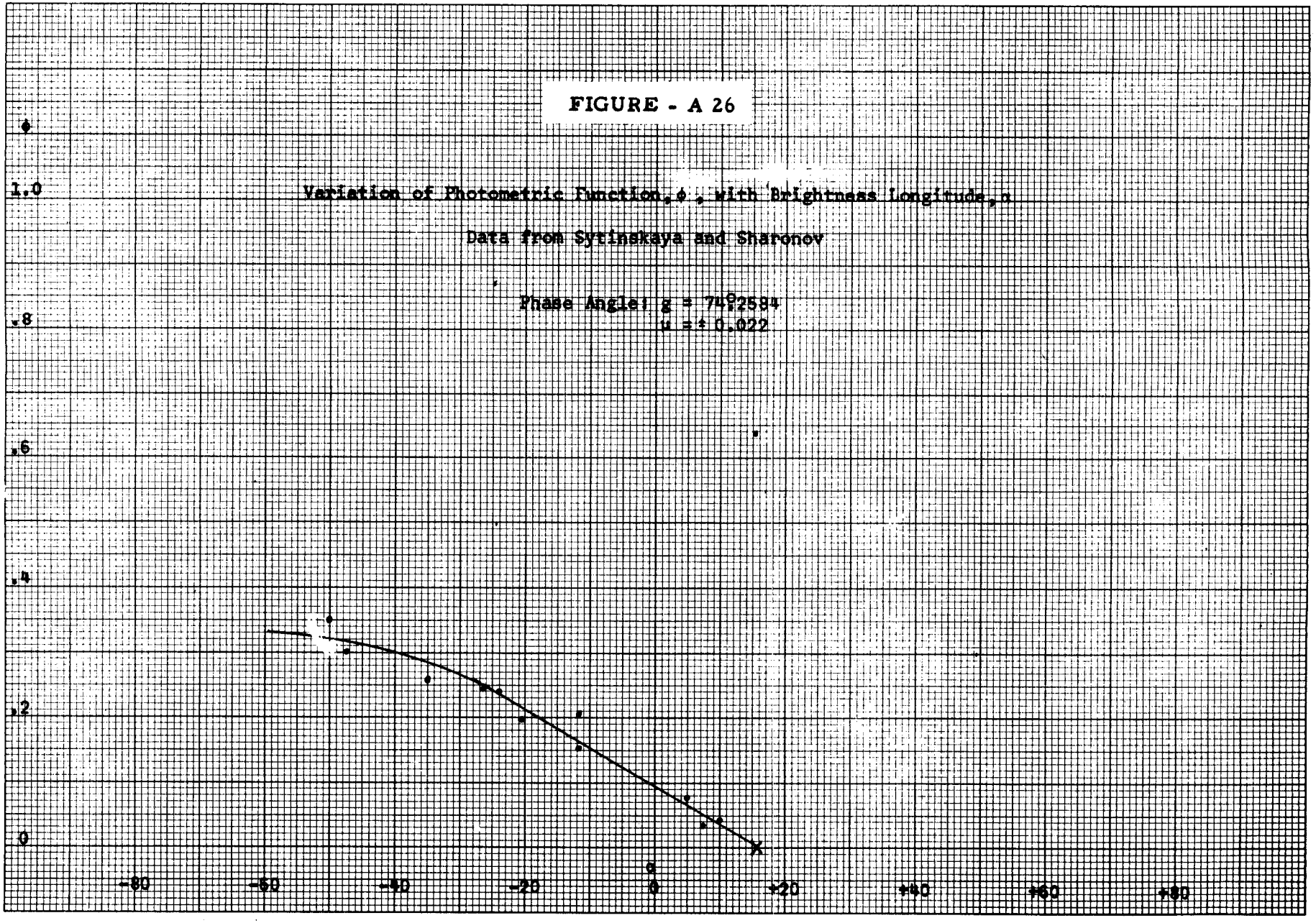
Variation of Photometric Function, Φ , with Brightness Longitude, α
Data from Sytinskaya and Sharonov
Phase Angle: g = 74°.2584
μ = ± 0.022
Φ
1.0
.8
.6
.4
.2
0
-80
-60
-40
-20
α
0
+20
+40
+60
+80

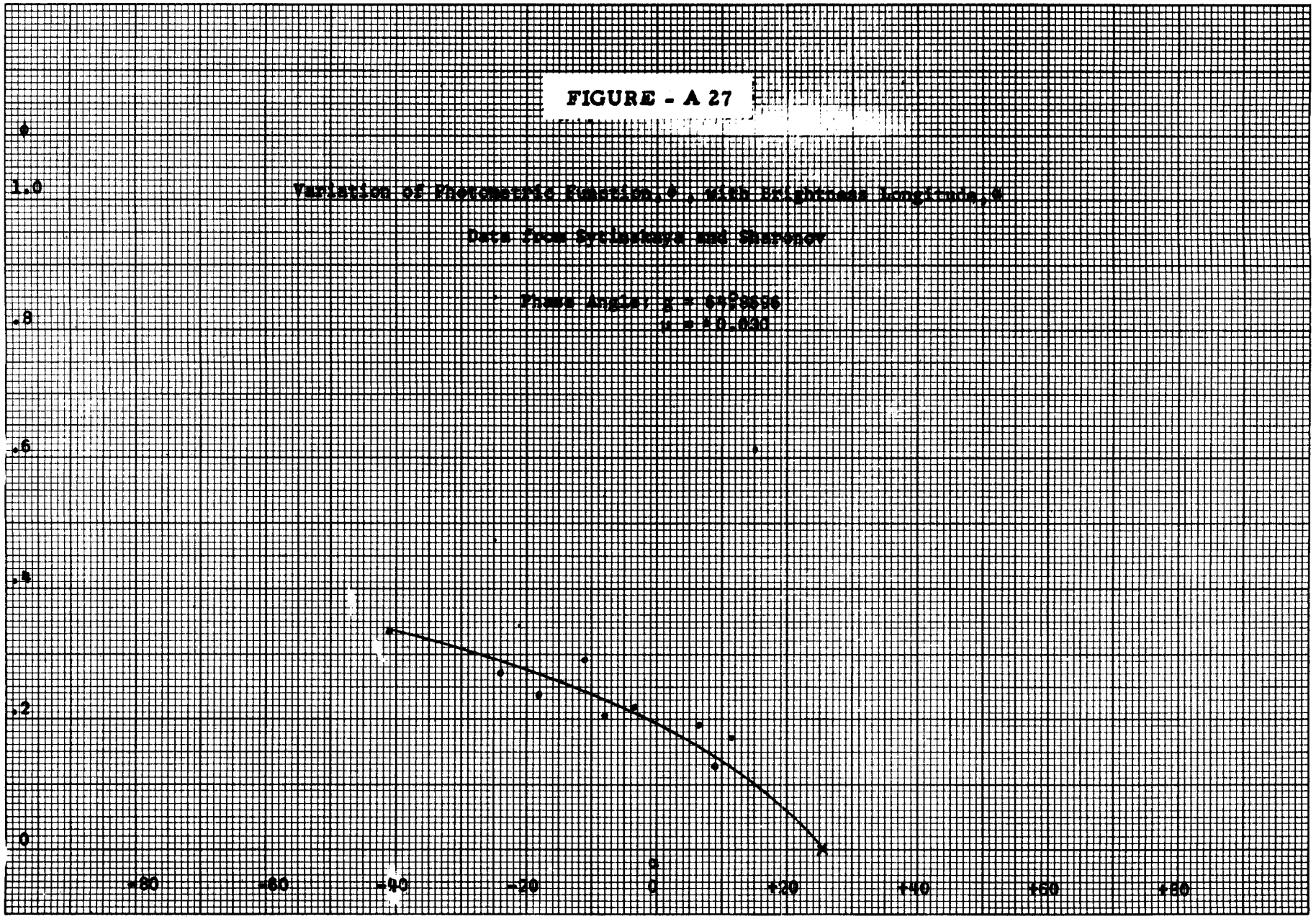
FIGURE - A 27
Variation of Photometric Function, Φ , with Brightness Longitude, ℓ
Data from Sytinskaya and Sharonov
Phase Angle: χ = 6°.9696
α = ±0.030
Φ
1.0
.8
.6
.4
.2
0
-80
-60
-40
-20
0
+20
+40
+60
+80
ℓ

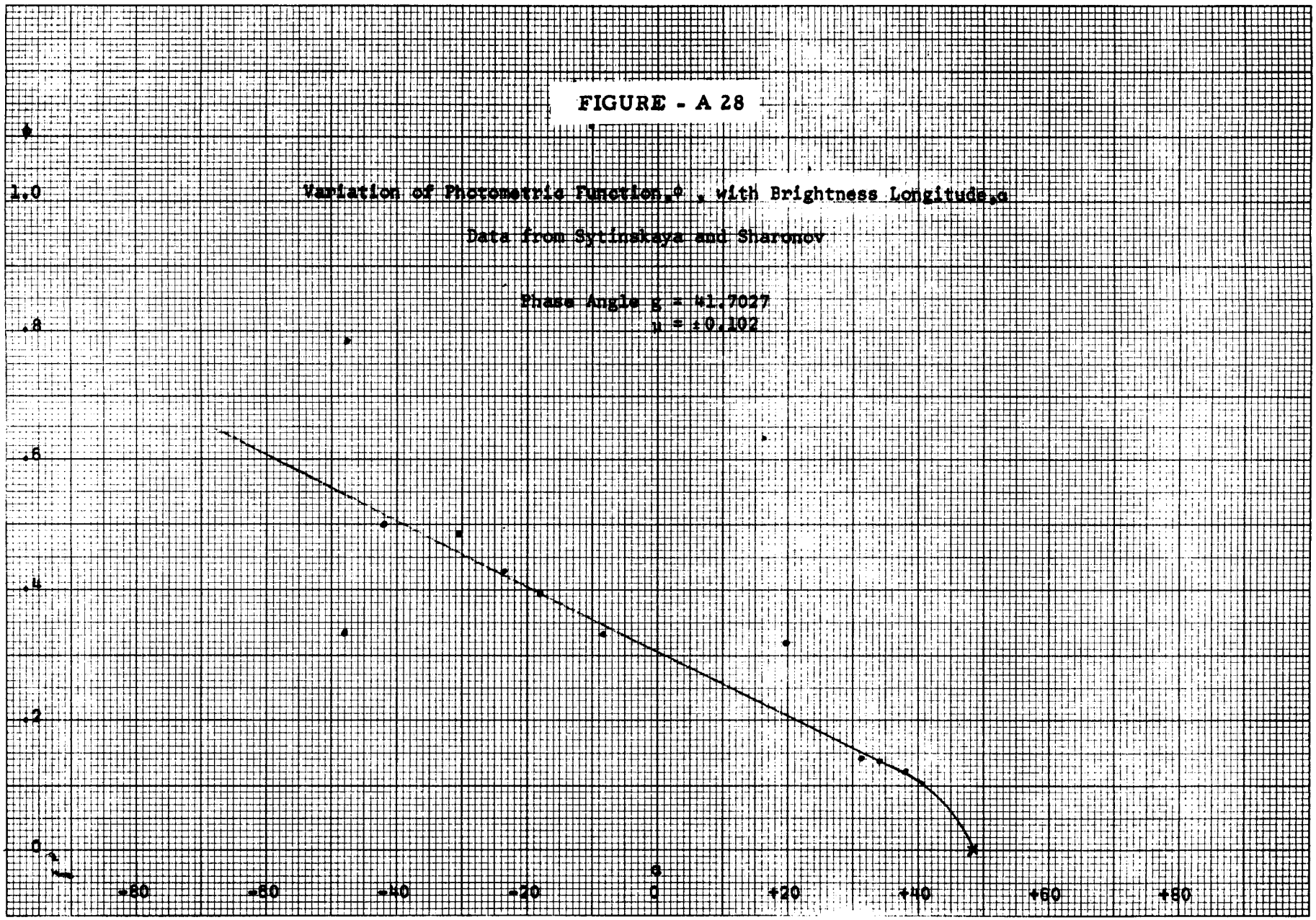
FIGURE - A 28
Variation of Photometric Function, Φ , with Brightness Longitude, a
Data from Sytinskaya and Sharonov
Phase Angle g = 41.7027
μ = ±0.102
1.0
.8
.6
.4
.2
0
-80
-60
-40
-20
0
+20
+40
+60
+80

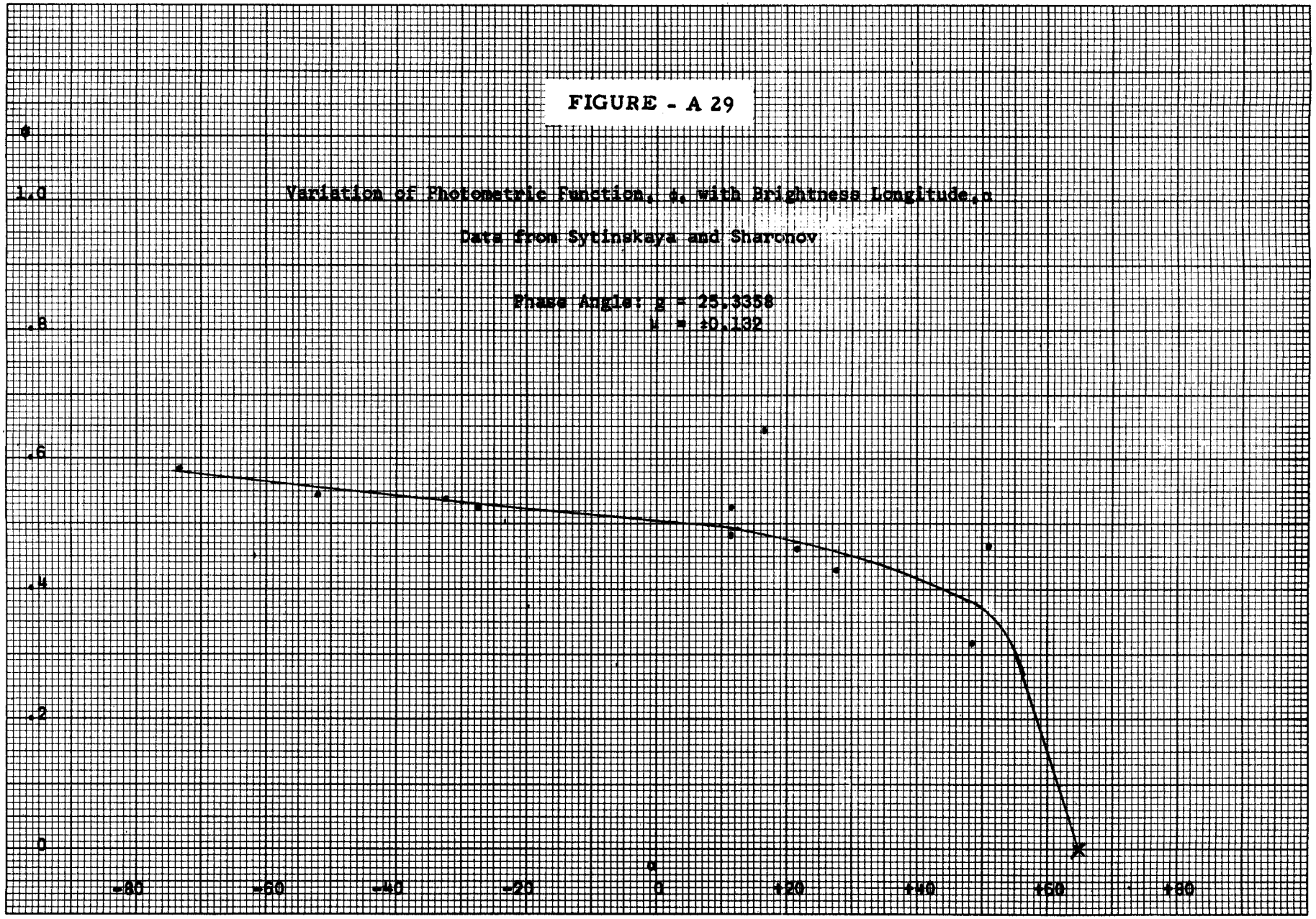
FIGURE - A 29
Variation of Photometric Function, ϕ_1, with Brightness Longitude, n
Data from Sytinskaya and Sharonov
Phase Angle: g = 25.3358
μ = ±0.132
ϕ
1.0
.8
.6
.4
.2
0
-80
-60
-40
-20
0
+20
+40
+60
+80

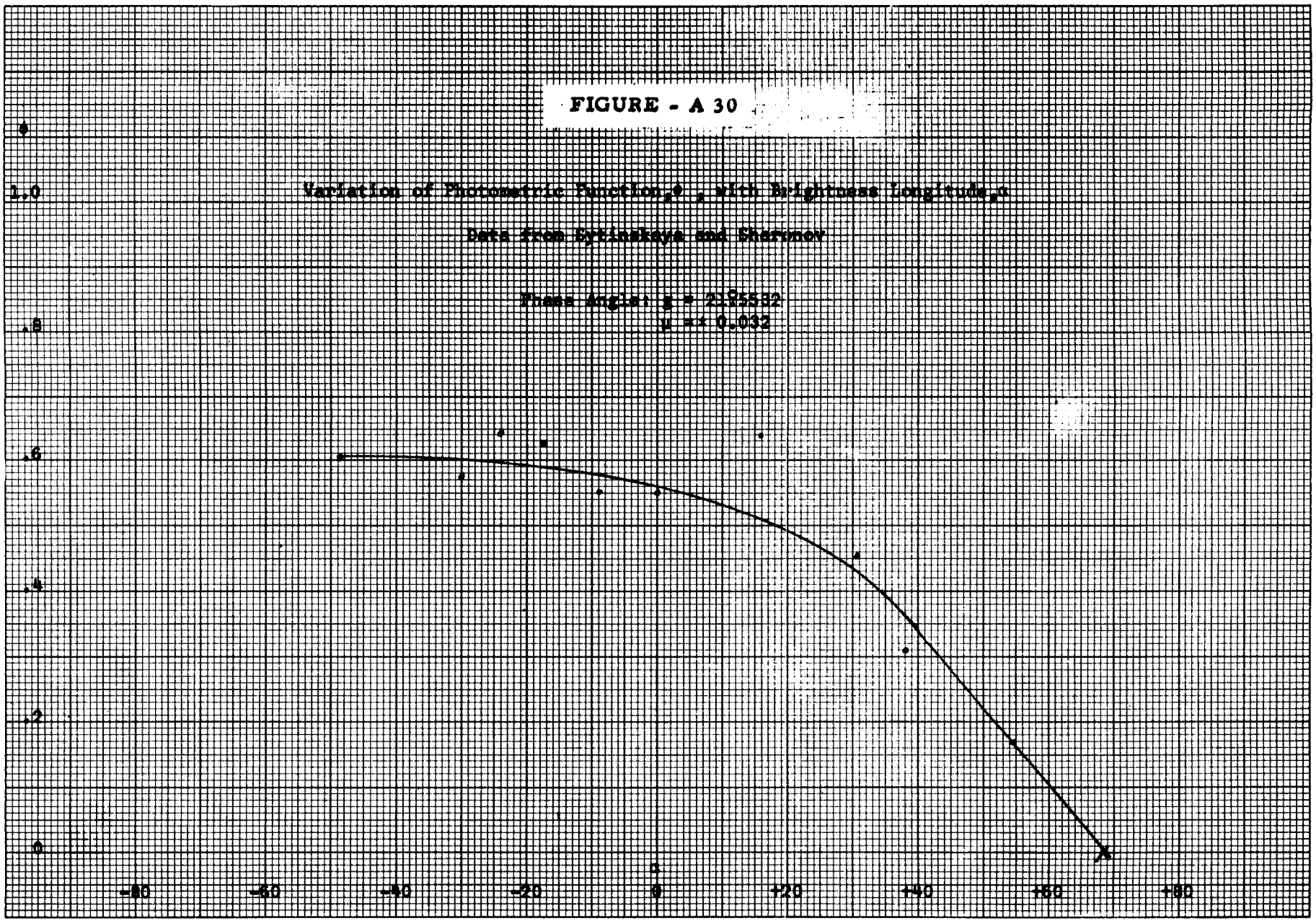
FIGURE - A 30
Variation of Photometric Function Φ_s with Brightness Longitude α
Data from Fytinskaya and Sharmov
Phase Angle: β = 2.1°55532
μ = ± 0.032
1.0
.8
.6
.4
.2
0
-80
-60
-40
-20
0
+20
+40
+60
+80

FIGURE - A 31

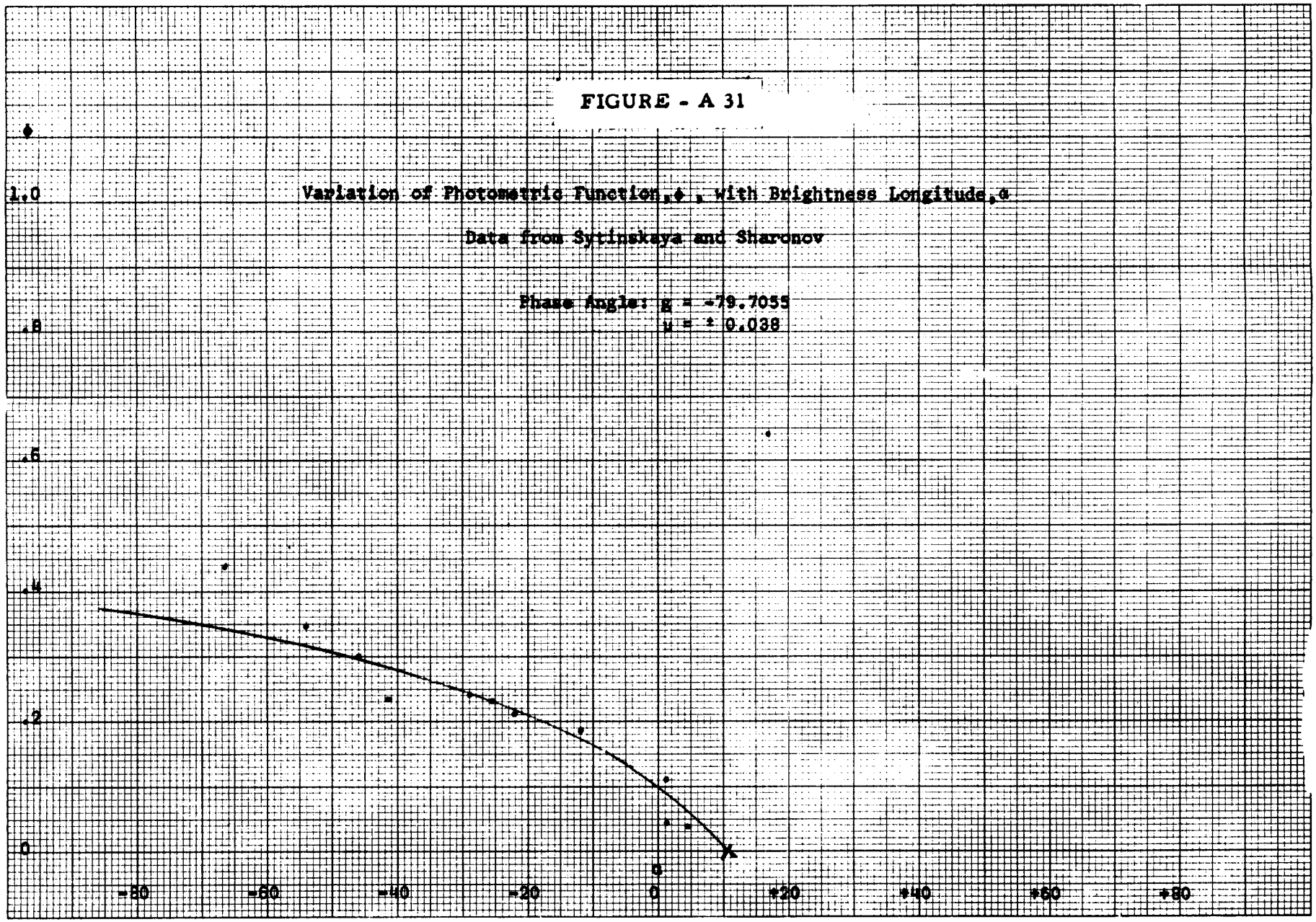
Variation of Photometric Function, Φ , with Brightness Longitude, α
Data from Sytinskaya and Sharonov
Phase Angle: g = -79.7055
μ = ± 0.038
Φ
1.0
.8
.6
.4
.2
0
-80
-60
-40
-20
0
+20
+40
+60
+80
α

DISTRIBUTION LIST

Copy No.	
1 - 25	Office of Grants and Research Contracts Code SC National Aeronautics and Space Administration Washington 25, D. C.
26 - 35	Mr. Archibald Sinclair Instrument Research Division Langley Research Center, NASA Langley Station Hampton, Virginia
36	T. T. Mayo
37 - 41	D. S. Birney
42	H. M. Parker
43	A. R. Kuhlthau
44	G. A. McAlpine
45 - 54	RLES Files